

# Sedimentary organic matter signature hints at the phytoplankton-driven Biological Carbon Pump in the Central Arabian Sea

Medhavi Pandey<sup>1,2</sup>, Haimanti Biswas<sup>1,2\*</sup>, Daniel Birgel<sup>3</sup>, Nicole Burdanowitz<sup>3</sup>, Birgit Gaye<sup>3</sup>

<sup>1</sup>CSIR National Institute of Oceanography, Biological Oceanography Division, Dona Paula, Goa 403004, India.

<sup>2</sup>Academy of Scientific and Innovative Research (AcSIR), Ghaziabad-201002, India.

<sup>3</sup>Institute for Geology, Center for Earth System Research and Sustainability (CEN), Universität Hamburg, Bundesstraße55, 20146, Hamburg, Germany.

\*Corresponding Author's email: [haimanti.biswas.nio@gmail.com](mailto:haimanti.biswas.nio@gmail.com); [haimanti.biswas@nio.org](mailto:haimanti.biswas@nio.org)

## Abstract

The Central Arabian Sea, a unique tropical basin is profoundly impacted by monsoon wind reversal affecting its surface circulation and biogeochemistry. Phytoplankton blooms associated with high biological productivity and particle flux occurs in the northern part of the central Arabian Sea due to summer monsoon-induced open ocean upwelling and winter convection. The core Oxygen Minimum Zone (OMZ) at the intermediate water depths is another important feature of the north-central Arabian Sea and fades southward. In this study, we have attempted to interlink how these factors collectively impact phytodetrital export to the sediment. Short sediment core top (1 cm) samples representing the recent particle flux signatures were analyzed from 5 locations (21° to 11° N; 64° E) in the central Arabian Sea. Previously, we were used only core top (0-0.5 cm) samples and we observed a trend between diatom frustule abundance and diversity with bulk sedimentary parameters indicating a spatial variability in phytodetrital export to the sediment. To strengthen verify this observation further fact, organic lipid biomarkers for of key phytoplankton groups and a sea surface temperature (SST) proxy have been analyzed in addition to diatom frustules. The C<sub>37</sub> alkenone-based ~~sea surface temperature (SST)~~ proxy indicated cooler SST (27.6 ± 0.25 °C) in the north (21–15° N) mostly due to upwelling (summer) and convective mixing (winter). ~~and Warmer SSTs (+0.4 °C) are measured~~ in the south, which usually remains nutrient-poor. This trend was consistent with ~~the~~ satellite-derived average SST values (2017–2020). Lipid biomarker analysis suggest ~~ed~~ that dinoflagellates were likely to be the highest contributor as indicated ~~in~~ by dinosterol and its degradative product dinostanol, followed by brassicasterol<sub>5</sub> and C<sub>37</sub> alkenone, likely representing diatoms ~~s~~<sub>5</sub> and coccolithophores, respectively. ~~The stations in~~ †The north (21–15° N), which that largely experiences periodic phytoplankton blooms and is influenced by the thick OMZ<sub>5</sub>, revealed the highest contents of organic matter, diatom frustules (diversity and abundance), dominated by large thickly silicified cells (e.g. *Coscinodiscus* and *Rhizosolenia*), and phytoplankton ~~organic-lipid~~ biomarkers, and as well as but lower contents of zooplankton biomarkers (cholesterol and cholestanol). ~~Whereas-In contrast,~~ relatively smaller chain-forming centric (e.g. *Thalassiosira*) and pennate (e.g. *Pseudo-nitzschia*, *Nitzschia*, *Thalassionema*) diatom frustules along with lower phytoplankton lipid biomarker contents were found in the south where zooplankton biomarkers and silicious radiolarians were more abundant. The ~~possible probable~~ impacts of ~~the presence of the~~ OMZ ~~along the sampling transect~~ on particle flux related to the phytoplankton community, including zooplankton grazing ~~along with and~~ other factors have ~~also~~ been discussed.

**Keywords:** Phytodetritus; North Indian Ocean; Monsoon; Biomarkers; Brassicasterol; Dinosterol

## 48 1. Introduction

49 Marine phytoplankton modulates the global carbon cycle by fixing almost 48 Gt C annually  
50 (Singh and Ahluwalia, 2013) which corresponds to 50% of the global primary production  
51 (Field et al., 1998; Behrenfeld et al., 2006). This amount of organic matter produced within the  
52 euphotic layers, where more than 1% of ~~solar~~ sunlight arrives, supports the entire marine food  
53 chain including the benthic population. Nearly 10% of this organic matter (large and dense  
54 phytodetritus) sinks to the upper mesopelagic ocean and gets further fragmented by  
55 zooplankton and microbially remineralized on its descent into the deep ocean. Only 1–3% of  
56 this phytodetritus can reach the seafloor below 1000 m water depth (Iversen, 2023) and can be  
57 stored for hundreds to millions of years (Buesseler, 1998), and is called sequestration flux. This  
58 way of trapping carbon from the atmosphere to the ocean interior mediated by phytoplankton  
59 is called the Biological Carbon Pump (BCP) (Volk and Hoffert, 1985; Le Moigne, 2019;  
60 Iversen, 2023 and references therein). However, the organic matter in the surface sediment can  
61 be further modified biogeochemically. The strength of BCP is governed by many factors, such  
62 as heterotrophic remineralization of organic matter, dissolved oxygen (DO) levels,  
63 temperature, phytoplankton community composition, cell size, and zooplankton activity  
64 (Marsay et al., 2015; Keil et al., 2016; Cavan et al., 2017; Engel et al., 2017; Iversen, 2023).  
65 Out of multiple factors controlling the efficacy of the BCP, phytoplankton community  
66 composition (that controls organic matter stoichiometry), zooplankton grazing (Cavan et al.,  
67 2017), and ~~the mid-water presence of well-oxygenated water~~ oxygen concentrations (Keil et al.,  
68 2016) are crucial factors. Thus, understanding the functioning of the marine BCP in productive  
69 marine ecosystems needs attention, particularly in the context of changing climate (Iversen,  
70 2023).

71 ~~Marine organic matter is preserved in sediments among others in the forms of as~~ Diatom  
72 frustules, dinoflagellate cysts, and ~~organic-lipid~~ lipid biomarkers (e.g. sterols, alkenones) preserved  
73 in sediments, which could be potential proxies for the reconstruction of productivity and  
74 understanding organic matter transport from the surface to the deep sea floor (Liu et al., 2013;  
75 Hu et al., 2020; Xiong et al., 2020 and references therein). The responses of phytoplankton to  
76 changing climate as well as other environmental variables can be retrieved from the sediments  
77 and may help predict future primary production, community shifts in marine ecosystems, and  
78 the ocean's role as a carbon sink. Generally, ~~T~~ the siliceous frustules of diatoms ~~can be~~ are  
79 more resistant to grazing and degradation and can be better preserved in sediments compared to other  
80 phytoplankton groups. Sedimentary organic carbon, nitrogen, and their ratios, diatom frustules,  
81 and ~~organic biomarkers~~ lipid biomarkers (e.g. sterols and alkenones) are used to reconstruct  
82 past phytoplankton community shifts and temperatures (Schubert et al., 1998; Liu et al., 2013;  
83 Rodríguez-Miret et al., 2023). The lipid biomarkers of phytodetritus from the surface sediments  
84 can also provide valuable information about the surface processes controlling phytoplankton  
85 growth and their transport to the sediment (Xiong et al., 2020). For example in a study by Peng  
86 et al. (2023), phytoplankton community shift was evident ~~in~~ from lipid biomarkers in the  
87 sediment core samples from the East China Sea. In a few studies, major phytoplankton-~~derived~~  
88 lipid biomarkers like dinosterol, brassicasterol, and alkenone were also used to correlate their  
89 contents with palaeoproductivity and associated changes of the sea ice levels in the Arctic  
90 Ocean (Müller et al., 2011, and references therein).

91  
92 The Arabian Sea, in the northwestern part of the Indian Ocean, is a unique marine province  
93 with several characteristic features, for instance, the direct influence of monsoon winds on  
94 oceanographic and biogeochemical processes, high productivity (McCreary et al., 2009), and  
95 one of the thickest (200–1200 m) oxygen minimum zones (OMZ) in modern oceans (Banse et  
96 al., 2014). The entire area experiences periodic reversals of monsoon winds and ~~in its~~ surface

97 circulation. During the summer (SW) monsoon, a low-level atmospheric ~~Jet-jet~~ (the Findlater  
98 Jet; Findlater, 1971) blows parallel to the Omani and Somalia coasts, generating coastal and  
99 open ocean upwelling in its northern part. Subsequently, due to natural nutrient enrichment,  
100 phytoplankton blooms develop (Banse, 1987; Bhattathiri et al., 1996; Prasanna Kumar et al.,  
101 2000). In the winter (NE) monsoon, winds and surface circulation reverse and in the northern  
102 Arabian Sea, the cooling and densification of surface water leads to convective mixing  
103 (Prasannakumar et al., 2001) that also fuels high phytoplankton growth (Madhupratap et al.,  
104 1996).

105  
106 In the Arabian Sea, the magnitude of particle transfer to the deep sea floor is directly controlled  
107 by the surface processes (Schulte et al., 1999, Rixen et al., 2019a). The central Arabian Sea  
108 exhibits one of the highest particle flux rates ( $1.3\text{--}3.3\text{ g C m}^{-2}\text{ year}^{-1}$ ) (Haake et al., 1993)  
109 compared with other low-latitude seas (Rixen et al., 2019b). This is mostly associated with  
110 enhanced biological productivity governed by summer monsoon-induced upwelling and winter  
111 convection (Nair et al., 1989; Haake et al., 1993; Rixen et al., 2019a). Nevertheless, particle  
112 flux could vary significantly (Nair et al., 1989; Prahl et al., 2000) during the intermonsoon and  
113 premonsoon due to prevailing oligotrophy (Prasanna Kumar and Narvekar, 2005).

114  
115 The impacts of atmospheric forcings and consequent biological response in the central Arabian  
116 Sea have been studied thoroughly during the joint Global Ocean Flux Studies (JGOFS, from  
117 1987 to 2003). ~~It was is evident that t~~The monsoon wind is the major controlling forcing of  
118 physical, chemical, and biological processes in the surface ocean (McCearry et al., 2009) with  
119 high spatial and seasonal variability (Prasanna Kumar and Narvekar, 2005). However, there  
120 ~~was ishas been~~ no further investigation in the last two decades, although ocean warming  
121 continued with high spatial variability (Roxy et al., 2016; Sharma et al., 2023 and references  
122 therein). Our previous study showed that diatom frustules retrieved from the surface sediments  
123 from the central (Pandey et al., 2023) and the eastern (Pandey and Biswas, 2023) Arabian Sea  
124 could be an efficient indicator of surface processes controlling euphotic phytoplankton  
125 communities. There are a few studies from the Arabian Sea characterizing sedimentary organic  
126 carbon using phytoplankton biomarkers (Schubert et al., 1998; Prahl et al., 2000; Schulte et al.,  
127 1999; 2000) suggesting such proxies from the surface sediment may be quite useful to  
128 understand the spatial variability in organic matter transport. Prahl et al. (2000) used  
129 phytoplankton biomarkers (e.g. C<sub>37</sub>-alkenones, dinosterol, 24-ethylethole $\beta$ -sitosterol) from  
130 sediment trap samples as well as from the surface sediments over a year from the central  
131 Arabian Sea (15°59'N, 61°30'E) and showed the seasonal variability ~~in surface water~~  
132 ~~conditions that modified of~~ biological productivity. Nevertheless, the degradation of organic  
133 matter in the water column could be quite high during their descent through the water column  
134 pointed out by Wakeham et al. (2002) in their work on lipids from the water column of the  
135 western Arabian Sea.

136  
137 Importantly, the Arabian Sea is warming at a faster pace compared to other oceanic regions  
138 (Roxy et al., 2016; Sharma et al., 2023), and how the phytoplankton-driven organic matter  
139 transport may respond to that change is still poorly understood. Furthermore, recent modeling  
140 studies (Vallivattathillam et al., 2023) as well as data from biogeochemical--aArgo floats (Liu  
141 et al. 2024) hinted ~~at the possibility of~~ at a possible thinning of the OMZ in the Arabian Sea  
142 that may substantially impact organic matter degradation within the water column, specifically  
143 in the southern part (Roxy et al., 2016). ~~--To fill this gap, in the present study,~~ we want to  
144 address three major questions in this study, -1) Which phytoplankton group dominates the  
145 sedimentary organic matter in the various stations of the transect from north to south? 2) Does  
146 high spatial variability in the phytoplankton community composition driven by physical

147 forcing also impact organic matter transport? 3) What are the possible factors (hydrography,  
148 physicochemical conditions, and atmospheric forcings) being responsible for such spatial  
149 variability in organic matter transport in this region? To address these questions, we have  
150 measured key parameters from surface sediments including lipid biomarkers, alkenone-based  
151 SST reconstruction, and diatom frustules combined with ~~a few our~~ recent in-situ observations  
152 on hydrography, biogeochemistry, and phytoplankton community from the central Arabian Sea  
153 (Silori et al., 2021; ~~2022~~; Chowdhury et al., 2021; Pandey et al., 2023; Chowdhury et al., 2024).  
154 In our previous study (Pandey et al., 2023) using the core top (0—0.5 cm)-same samples (only  
155 the core to 0-0.05 cm)-we observed a trend between diatom frustules abundance and diversity  
156 with sedimentary parameters and atmospheric forcings. In this study, lipid biomarkers of other  
157 phytoplankton groups including diatoms are considered to understand their contribution to  
158 organic matter flux. Further, a lipid biomarker as an SST proxy has also been studied to  
159 correlate with atmospheric forcingslipid.

## 161 2. Methodology

### 162 2.1. Sample collection

163  
164 During cruise SSD-068 (Dec 2019 to Jan 2020) with *RV. Sindhu Sadhana* five short sediment  
165 cores were obtained using a multicorer (Ocean Scientific International Limited Maxi Multi-  
166 corer; core tubes 60 cm, outer diameter 11 cm and 10 cm inner diameter) along a transect from  
167 11–21° N at 64° E (Fig. 1a). These short cores were collected at 21° N, 19° N, 15° N, 13° N,  
168 and 11° N with varying water depths between 3000 m and –4500 m (Fig. 1a). The cores were  
169 subsampled onboard immediately at everyin 0.5 cm slices-down-to-the-core and were kept in  
170 pre-cleaned plastic containers at 0–4 °C. The advantage s-of using a multicorer is the-a better  
171 preservation of the topmost parts of the sediment core compared to other devices like box or  
172 gravity coring (Barnett et al., 1984). For this study, we used the top 1 cm (0-0.5 cm and 0.5-1  
173 cm; slices-1) of the cores for all related analyses. Note that the core top samples (0—0.5 cm)  
174 were analysed for total inorganic carbon (TIC), total organic carbon (TOC), total nitrogen  
175 (TN) as well as diatom frustules and diversity including radiolarian abundance earlier by  
176 Pandey et al.; (2023).

### 177 178 2.2. Analytical method

#### 179 2.2.1. Total inorganic carbon (TIC), total organic carbon (TOC), and total nitrogen (TN) 180 contents

181 For this study, Ss Sediment samples (0.5—1 cm) were dried at 60 °C overnight and ground  
182 using agate mortar and pestle. Aliquots (10 mg) of sediment samples were taken in tin capsules.  
183 Total carbon (TC) and TN were measured using a CHN Elemental analyzer (Euro Vector  
184 EA3000 series analyzer) at the Central Analytical Facility of CSIR-National Institute of  
185 Oceanography, Goa, India) against soil reference material NC soil standard (5g 338 40025  
186 procured from Elemental Microanalysis Ltd, UK, Soil Standard Clay OAS Cat No. B2051-  
187 Certificate No. 341506) used for carbon and nitrogen (ThermoFisher Scientific, Cambridge,  
188 UK) with an analytical error of < 2%. The TIC contents were measured against the calcium  
189 carbonate (CaCO<sub>3</sub>) standard (Merck, Germany) in a coulometer attached to an acidification  
190 module (Model CM5015 (UIC, USA). The accuracy and precision obtained from the results  
191 were within ± 1.25%. TOC values were calculated by the difference between TC and TIC (TOC  
192 =TC-TIC).

#### 193 2.2.2. Analysis of silica-bearing organisms from sediments

194 The diatom frustules and other siliceous organisms from sediments (0.5—1 cm) were  
195 enumerated following the method by Armbrrecht et al. (2018). The dried sediment subsamples  
196 (50 mg) were taken in a 150 mL sterile polypropylene tube and were treated chemically with  
197 10% HCl, 30% H<sub>2</sub>O<sub>2</sub>, and 0.01 N anhydrous sodium diphosphate (Na<sub>4</sub>P<sub>2</sub>O<sub>7</sub>) for removing  
198 carbonate, organic matter, and fine clay, respectively. After each chemical treatment, samples  
199 were washed ~~three times~~ ~~thrice~~ with 15 mL Milli-Q water. Finally, the residue remaining after  
200 the last rinse and decantation was diluted with Milli-Q to 10 mL and was homogenized. A  
201 small portion (1 mL) from this homogenized solution was analyzed under an inverted  
202 microscope (Nikon Ti2) in a Sedgewick rafter counting chamber (Pysen, UK) at 400–600×  
203 magnification. The classical identification keys by Tomas (1997), Desikachary (1989), and  
204 <http://www.algaebase.org> were used. No centrifugation was used in this process to ~~restrict~~  
205 ~~avoid~~ the breaking of frustules. Further, the diatoms more than half in size were considered  
206 complete valves (Abrantes and Sancetta, 1985). The diatom abundance was expressed as valves  
207 g<sup>-1</sup> dry sediment. Radiolarians were also enumerated along with diatom frustules ~~and given and~~  
208 ~~were represented~~ as individuals g<sup>-1</sup>.

### 209 2.2.3 Biomarker analysis and SST temperature proxy

210 Lipid biomarker analyses were carried out at the Institute for Geology, University of Hamburg,  
211 Germany. About 11 g to 19 g of freeze-dried and ground samples were used to obtain total lipid  
212 extracts (TLEs) by using an Accelerated Solvent Extractor (ASE200, DIONEX). Before  
213 extraction, a known amount (10 ng μL<sup>-1</sup>) of internal standards (14-heptacosanone,  
214 nonadecanol, and dialkylglycerol ether-18 (DAGE-18)) were added to the samples. The ASE  
215 extraction for each sample was carried out at 100°C and 1000 PSI for 5 minutes in 3 cycles by  
216 using the solvent mixture dichloromethane: methanol (DCM: MeOH, 9:1). The TLEs were  
217 then concentrated with rotary evaporation and were separated later into a hexane-soluble  
218 (adding *n*-hexane) and hexane-insoluble (adding DCM) fraction via NaSO<sub>4</sub> column  
219 chromatography. To separate the hexane-soluble fraction into a neutral- and acid fraction via  
220 saponification (at 85°C for 2 hrs) a 5 % potassium hydroxide (KOH) in MeOH solution was  
221 added to this fraction. Then, the neutral fractions were obtained by adding *n*-hexane to the  
222 saponified fraction, vortexing, and pipetting the neutral fraction containing *n*-hexane layer into  
223 a new vial. The neutral fractions were then separated into apolar-, ketone- (containing  
224 alkenones), and polar fractions (containing sterols, stanols) by column chromatography packed  
225 with deactivated silica gel (5 % H<sub>2</sub>O, 60 μm mesh) using the solvents *n*-hexane, DCM, and  
226 DCM: MeOH (1:1), respectively. We took 50% splits of the ketone- and polar fractions and  
227 put them together, as some of the sterols and added standards for the sterol fraction were found  
228 in the ketone fraction, too. For the derivatization of these fractions, a mixture of 200 μL  
229 BSTFA: Pyridin (1:1) was added to the dried sample and heated at 80°C for 2 hrs followed by  
230 drying under an N<sub>2</sub> environment.

231 To quantify the alkenones and sterols the samples were measured with a Thermo Scientific  
232 Trace 1310 gas chromatography coupled to a flame ionization detector (GC-FID) equipped  
233 with a Thermo Scientific TG-5MS column (30 m, 0.25 mm, 0.25 μm). H<sub>2</sub> as carrier gas was  
234 used with a flow rate of 35 mL minute<sup>-1</sup> and the PTV injector started at 50°C ramped with  
235 10°C/s to 325°C in a splitless mode. For the alkenones, the initial GC temperature was  
236 programmed to 50°C (held 1 minute) and then ramped to a temperature of 230 °C with an  
237 increased rate of 20 °C minute<sup>-1</sup>, then increased ~~with-at~~ 4.5°C minute<sup>-1</sup> to 260 °C, and ~~finally~~  
238 ~~increased the temperature withat~~ 6 °C minute<sup>-1</sup> to 325 °C, which was held for 15 minutes. The  
239 peaks of alkenones were identified by comparing the retention time for peaks of the samples  
240 with a known working sediment standard. Quantification of the alkenones was done by using  
241 14-heptacosane and tetratriacontane with a known amount (10 ng μL<sup>-1</sup>) as external standards.  
242 Repeated measurements of the external standards yielded a quantification precision of 13 %

243 (14-heptacosanone) and 8 % (tetratriacontane). The alkenone saturation index was calculated  
244 using the equation by Prahl et al. (1988):

$$245 \quad U_{37}^{k'} = \frac{C_{37:2}}{C_{37:2} + C_{37:3}}$$

246 to convert the  $U_{37}^{k'}$  index to SSTs we have used the core top calibration of Indian Ocean  
247 sediments (Sonzogni et al., 1997):

$$248 \quad SST = \frac{U_{37}^{k'} - 0.043}{0.033}$$

249 For each sample, at least a duplicate measurement was conducted, which yielded an average  
250 precision of 0.1°C (1SD). Replicate extractions of a working standard sediment (n=2) and its  
251 duplicate measurements ~~of where~~ each replicate yielded ~~to~~ an average precision of 0.5°C (1  
252 SD).

253 For the quantification of the sterols, the initial GC temperature was 50°C (held for 3 minutes)  
254 and then programmed to a final temperature of 325 °C (held for 20 minutes) with an increase  
255 of 6 °C minutes<sup>-1</sup>. To quantify the sterols we used nonadecanol and DAGE-18 with a known  
256 amount (10 ng µL) as external standards, with precision of 5.6 % and 4.9 %, respectively. To  
257 identify the sterols the mass spectra of each sample were investigated using a Thermo Scientific  
258 Trace GC Ultra coupled to a Thermo Scientific DSQ II mass spectrometer (GC-MS). He (2 mL  
259 minute<sup>-1</sup> flow rate) was used as carrier gas. The initial GC temperature was 50 °C (held for 3  
260 minutes) and ramped with 6 °C minute<sup>-1</sup> to 325 °C (held for 25 minutes). The mass spectra of  
261 the compounds were then compared with published mass spectral data.

262 ~~For major four phytoplankton groups, (brassicasterol, dinosterol, dinostanol and C<sub>37</sub>-alkenone)~~  
263 ~~were are used. For zooplankton cholesterol, and its degradative product cholestanol~~  
264 ~~(Wittenborn et al., 2020) wasare used.~~

#### 265 **2.2.4 Sea surface temperature (SST) and Chlorophyll a (Chla) from satellite imagery**

266 The SST data was accessed from the climate reanalysis version 5 (ERA5) of the European  
267 Centre for Medium-Range Weather Forecasts (ECMWF) (C3S, 2017). ERA5 covers the time  
268 from 1979 to the present at a 0.25° × 0.25° grid. In this study, we used monthly mean of SST  
269 data averaged for covering—a period from 2017–2020 (downloaded from:  
270 <https://cds.climate.copernicus.eu/cdsapp#!/dataset/reanalysis-era5-single-levels?tab=form>.  
271 Chla values were derived from Aqua MODIS at a 4 km resolution. The average was calculated  
272 from daily Chla data during the period of 2017 Jan to 2020 Dec (downloaded from  
273 <https://oceancolor.gsfc.nasa.gov/13/>).

#### 274 **2.2.5 Statistical analysis**

275 The Shapiro-Wilk normality test and F test were used to check the normality and variance of  
276 individual datasets, respectively. The statistical significance between differences for various  
277 parameters was obtained using Singlesingle-factor Analysis of Variance (ANOVA) in  
278 Microsoft Excel 2019 at a 95% confidence level (probability  $p < 0.05$ ). The correlations between  
279 the biotic and environmental variables were derived using a linear multivariate model RDA  
280 (Redundancy Analysis). The relationships between the key variables (biomarkers, frustules,  
281 radiolarian, diatom community, TOC, TN, TOC: TN, TIC, and SST) are tested -using the  
282 CANOCO version 4.5 software (Ter Braak and Šmilauer, 2002). In this test, cluster I contained  
283 biomarkers, frustules, radiolarian, and diatom community, and cluster II included other  
284 variables and environmental (SST, TOC, TN, TIC, TOC: TN). ~~variables were conducted using~~  
285 ~~the CANOCO version 4.5 software (Ter Braak and Šmilauer, 2002). For explaining the~~

286 correlation between the biotic and environmental variables a linear multivariate model RDA  
287 (Redundancy Analysis) was used.

### 288 3. Results

289 The sedimentary characteristics (TIC, TOC, TN), diatom frustule abundance, and diversity  
290 including radiolarian abundance from this study (0.5–1 cm depth) and by (Pandey et al., 2023,  
291 core top 0–0.5 cm) the top 0–0.5 cm were already published earlier (Pandey et al., 2023). In  
292 this study, we have analyzed the samples from 0.5–1 cm sediment depth and collectively are  
293 shown as an average representing the top 1 cm of the surface sediment (Table 1). Results of  
294 lipid biomarkers (0–0.5 and 0.5–1 cm) such as various phytosterols and the summed C<sub>37:2</sub> and  
295 C<sub>37:3</sub> alkenones as well as U<sub>37<sup>k</sup></sub>-derived sea surface temperatures (SSTs) proxy are shown  
296 in Table 1. For further discussion of our results, the study area has been defined in as two areas:  
297 a as the northern part (north of the mean position of Findlater Jet) including the sites 21  
298 °N, 19 °N, and 15° N; whereas the and a southern part includes consists including of the sites  
299 11 °N, and 13 °N (Fig. 1a).

#### 300 3.1 Bulk sedimentary analysis and SST reconstruction

301 To compare with U<sub>37<sup>k</sup></sub> based-SST reconstruction, we also present here the SST values derived  
302 from the satellite data (Fig. 1b) averaged for the last three years (2017–2020). Assuming  
303 that the surface sediment usually represents the signature of recent time modern SST. High  
304 spatial variability in SST was is observed from the north (mean 27.24 °C) to the south (28 °C).  
305 To compare the average phytoplankton biomass distribution associated with cooler SSTs from  
306 the north to south, the surface chlorophylla (Chla) value average from 2017–2020 is shown  
307 in Fig. 1c. A distinct north-south variability is noticed with higher Chla values (~1–2 mg m<sup>-3</sup>)  
308 in the north and lower values in the south (~0–0.5 mg m<sup>-3</sup>). TIC contents (Fig. 2a) we are slightly  
309 higher in the south (7.06 ± 0.63 %) compared to the north (5.15 ± 1.57 %) and this difference  
310 was is statistically significant at a 94.7 % confidence level (single factor ANOVA analysis,  
311 Table 2). TOC contents (Fig. 2b) were are substantially higher (p < 0.001) above 15° N (0.97 ±  
312 0.06 %) reaching their highest value at 21° N and decreased southward (0.78 ± 0.005 %). TN  
313 values (Fig. 2c) revealed a similar trend as TOC and decreased from 21° N (0.11 ± 0.001 %)  
314 to 11° N (0.07 ± 0.009 %). The average TN value (0.06 ± 0.008 %) in the south was is  
315 significantly lower (p < 0.001) compared to the north (0.087 ± 0.018 %). The ratio of TOC and  
316 TN (Table 1) was is the lowest (9.5 ± 0.18) in the north at 21° N and increased at the rest of  
317 the stations reaching >12. The U<sub>37<sup>k</sup></sub> based SST (Fig. 2d) shows an average value of 27.8 ± 0.3  
318 °C. The coolest reconstructed SSTs (27.6 ± 0.25 °C) were are found in the north and were are  
319 nearly 0.4 °C cooler compared to the south (p ≤ 0.0543) (Table 2).

#### 320 3.2 Lipid biomarkers

321 The lipid biomarkers brassicasterol (diatoms) (Fig. 2e), dinosterol (dinoflagellates) (Fig. 2f),  
322 dinostanol, the saturated, degradative product of dinosterol (Fig. 2g), and summed C<sub>37:2</sub> and C<sub>37:3</sub>  
323 alkenones (C<sub>37</sub> alkenone) (eoccolithophores) (Fig. 2h), cholesterol (Fig. 2i), and its degradative  
324 product cholestanol (Fig. 2j) we are present in the surface sediments from north to south.

325 Among phytoplankton lipid biomarkers, the average dinosterol contents (98 ± 64 ng g<sup>-1</sup>)  
326 found in the surface sediment were are the highest of the biomarkers followed by brassicasterol  
327 (64 ± 44 ng g<sup>-1</sup>) and finally then C<sub>37</sub> alkenones (39.4 ± 12 ng g<sup>-1</sup>) (Table 1) and. All studied  
328 lipid biomarkers showed significant linear positive correlations (R<sup>2</sup> = 0.62–0.96, p < 0.05) with  
329 each other. All three biomarkers indicating their similar responses to environmental variables.  
330 Brassicasterol, dinosterol, dinostanol and alkenones. They show the highest concentrations  
331 we are quite high at the northernmost station at 21° N (Fig. 2; Table 1) and decreased to their  
332 minimum values at 11° N. In contrast, cholesterol and cholestanol are showing, on average,

333 higher concentrations at the southern stations compared to the northern stations (Fig. 2, Table  
334 1).

335 However, there were apparent trends of decrease from north to south of the sampling transect,  
336 but none of the biomarkers showed any statistically significant difference in their TOC  
337 normalized values between the stations. The sum of the major biomarkers (brassicasterol,  
338 dinosterol, and alkenones) grossly representing the major three phytoplankton groups, with the  
339 highest concentrations of phytoplankton related lipids (include reference) brassicasterol,  
340 dinosterol, dinostanol and alkenones ( $33.9 \pm 14.13 \mu\text{g g}^{-1} \text{TOC}$ ) occur at  $21^\circ \text{N}$  compared to  
341 other stations ( $19.96 \pm 9.5 \mu\text{g g}^{-1} \text{TOC}$ ) (Fig. 2). The TOC normalized values of dinosterol  
342 ( $16.53 \pm 8.3 \mu\text{g g}^{-1} \text{TOC}$ ) and brassicasterol ( $12.37 \pm 5.2 \mu\text{g g}^{-1} \text{TOC}$ ) were the highest at the  
343 northernmost station and decreased southward. However, the average values of  
344 dinosterol (north:  $12.81 \pm 6.3 \mu\text{g g}^{-1} \text{TOC}$ ; south  $7.8 \pm 4.47 \mu\text{g g}^{-1} \text{TOC}$ ) and brassicasterol  
345 (north:  $8.64 \pm 4.75 \mu\text{g g}^{-1} \text{TOC}$ ; south  $5.81 \pm 3.48 \mu\text{g g}^{-1} \text{TOC}$ ) were not significantly different  
346 ( $p > 0.05$ ) (Table 2). The average ratios of dinosterol to brassicasterol and brassicasterol to  
347 alkenones were 1.5 and 1.6 (Table 1), respectively, without any significant north-south  
348 variability (Table 2). However, none of the biomarkers showed any statistically significant  
349 difference in their TOC normalized values between the stations.

### 3.3 Zooplankton proxies

351 We used two proxies representing zooplankton: 1) sterol biomarker (cholesterol (Fig. 2i), and  
352 its degradative product cholestanol (Fig. 2j)), although it may come derive from some other  
353 sources (Wittenborn et al., 2020) and 2) radiolarians. Cholesterol (Fig. 2i), mostly varied  
354 between  $10 \pm 2.5 \mu\text{g g}^{-1} \text{TOC}$  (north) and  $14.3 \pm 5.8 \mu\text{g g}^{-1} \text{TOC}$  (south) without any statistical  
355 significance. The TOC normalized values of cholestanol (Fig. 2j) are lower in the northern  
356 ( $11.8 \pm 6.3 \mu\text{g g}^{-1} \text{TOC}$ ) than in the southern part ( $15.9 \pm 11.4 \mu\text{g g}^{-1} \text{TOC}$ ) and no significant  
357 correlation was noticed (Table 2).

358 Radiolarian abundance (Fig. 2k) in the central Arabian Sea varied between  $1.07$  and  $2.13 \times 10^4$   
359 individuals  $\text{g}^{-1}$  with the highest numbers at  $13^\circ \text{N}$  and the lowest at  $21^\circ \text{N}$ . Their occurrences  
360 were found to be higher at the southern stations ( $1.84 \times 10^4$  individuals  $\text{g}^{-1}$ ) compared to  
361 northern stations ( $1.10 \times 10^4$  individuals  $\text{g}^{-1}$ ) with statistical significance ( $p < 0.014$ ) (Table 2).  
362 The community was dominated by the genus *Tetrapyle* sp. and their abundance was higher in  
363 the south.

### 3.3.4 Silicious organisms: Radiolarians and Diatoms frustules: abundance and diversity

365 Radiolarian abundance (Fig. 2k) in the central Arabian Sea varied between  $1.07$  and  $2.13 \times 10^4$   
366 individuals  $\text{g}^{-1}$  with the highest numbers at  $13^\circ \text{N}$  and the lowest at  $21^\circ \text{N}$ . Their occurrences  
367 are found to be higher at the southern stations ( $1.84 \times 10^4$  individuals  $\text{g}^{-1}$ ) compared to northern  
368 stations ( $1.10 \times 10^4$  individuals  $\text{g}^{-1}$ ) with statistical significance ( $p < 0.05$ ) (Table 2). The  
369 community is dominated by the genus *Tetrapyle* sp. and their abundance was higher in the  
370 south.

371 Diatoms frustules from the surface sediments showed high spatial variability in both abundance  
372 and diversity. The total frustule abundance in the central Arabian Sea (Supplementary Table 1;  
373 Fig. 2l) ranged between  $2.78$  and  $6.36 \times 10^4$  valves  $\text{g}^{-1}$ . The highest frustule abundance was  
374 observed at  $19$ – $21^\circ \text{N}$  and the least at  $11^\circ \text{N}$ . At station  $19^\circ \text{N}$ , the frustule abundance was the  
375 highest ( $6.36 \pm 0.2 \times 10^4$  valves  $\text{g}^{-1}$ ) among all stations (Table 1). The frustule numbers found  
376 in the north ( $5.46 \pm 0.95 \times 10^4$  valves  $\text{g}^{-1}$ ) were 1.67 times higher than in the south  
377 ( $p \leq 0.0199$ ). Diatom frustule diversity has been calculated to understand the north-south  
378 distribution pattern and the average Shannon–Wiener diversity index ( $H'$ ) was  $1.6 \pm 0.1$  with  
379 the highest diversity at  $21^\circ \text{N}$  (1.8) (Supplementary Fig. 1). Microscopic analysis revealed a



380 total of 23 genera, with 9 centric and 14 pennate diatoms. More than five-fold higher abundance  
381 of centric diatoms ~~was is~~ observed than pennate at all the locations ( $p < 0.05$ ). ~~The abundance~~  
382 ~~of pennate diatoms was higher towards southern stations without any statistical significance.~~

383 The overall diatom community in the sediment samples from the central Arabian Sea  
384 (Supplementary Table 1; Fig. 3) ~~was is~~ observed to be dominated by *Coscinodiscus* (40%),  
385 *Thalassiosira* (34%), *Pseudo-nitzschia* (6%), *Rhizosolenia* (4%), *Hemidiscus* (4%),  
386 *Thalassionema* (4%), and *Nitzschia* (3%). The northern stations ~~were are~~ dominated by  
387 *Coscinodiscus* sp., whereas the two southernmost stations ~~were are~~ dominated by *Thalassiosira*  
388 sp. In the north, the highest abundance ( $2.46 \times 10^4$  valves  $g^{-1}$ ) of *Coscinodiscus* sp. was  
389 observed ( $p < 0.05$ ) with the least abundance at  $11^\circ$  N ( $0.61 \times 10^4$  valves  $g^{-1}$ ). In the south,  
390 *Thalassiosira* seemed to dominate ( $1.59 \times 10^4$  valves  $g^{-1}$ ) without any statistical significance.  
391 The Bray-Curtis similarity index usually indicates the similarity in the distribution pattern of  
392 different diatom genera/species. The results revealed (Supplementary Fig. 2) that the two  
393 dominating diatom genera, i.e. *Coscinodiscus* sp. and *Thalassiosira* sp. ~~were are~~ grouped  
394 showing a similar distribution pattern. The commonly occurring pennate diatom *Pseudo-*  
395 *nitzschia* ~~was is~~ present independently, whereas, *Rhizosolenia* and *Thalassionema* ~~are were~~  
396 ~~elubbedgrouped~~. The other two major contributing diatom genera, *Hemidiscus* and *Nitzschia*  
397 revealed a similar pattern.

### 398 **3.45 Statistical Analysis**

399 In the RDA biplot (Fig. 4), Axis 1 and 2 explained most of the variability (~97.2%). The biotic  
400 variables and ~~abiotic variables all other environmental parameters~~ show a distinct association.  
401 Interestingly, TOC, TN, the key phytoplankton biomarkers (dinosterol, brassicasterol,  
402 dinostanol, and alkenones), along with diatom frustules abundance, and the major genera ~~were~~  
403 ~~are elubbed-grouped~~ and ~~were are~~ at the opposite axis where TIC, SST, cholesterol, and  
404 radiolarian were together. The association between the larger diatoms like *Coscinodiscus* and  
405 *Rhizosolenia* and organic matter including brassicasterol ~~depicted depicts~~ that the organic  
406 matter flux ~~wais~~ coupled with diatom fluxes. The positioning of *Thalassiosira* opposite these  
407 parameters also suggests ~~ed~~ that its abundance ~~wais~~ higher in the south associated with warmer  
408 SSTs. TOC: TN ratio and TIC along with SST ~~we are together found to be closely related in the~~  
409 ~~RDA plot (Fig. 4).~~

## 410 **4. Discussion**

### 411 **4.1 Lipid biomarkers as indicators for phytoplankton and zooplankton**

412 ~~Phytoplankton and zooplankton produce specific lipid biomarkers stored in the oceans~~  
413 ~~sediments (e.g. Castañeda & Schouten, 2011; Meyer 1997; Volkman et al., 1998;~~  
414 ~~Volkman 2002) and are often commonly used to reconstruct environmental changes in the~~  
415 ~~past (e.g. Castañeda & Schouten, 2011, Eglinton & Eglinton, 2008). For instance, the~~  
416 ~~phytoplankton related coccolithophorids *Gephyrocapsa huxleyi* (also known as *Emiliana*~~  
417 ~~*huxleyi*) and *Gephyrocapsa oceanica* are known to be the main producers of  $C_{37}$ -alkenones in~~  
418 ~~the ocean (e.g. Brassell et al., 1986; Castañeda & Schouten, 2011; Eglinton & Eglinton,~~  
419 ~~2008; Prahl & Wakeham, 1987). The  $C_{37:2}$  and  $C_{37:3}$ -alkenones are highly used as SST~~  
420 ~~proxy in modern and past climate studies (e.g. Prahl et al., 1988; Sonzogni et al., 1997). The~~  
421 ~~sterol dinosterol and its degradative product dinostanol are often used as proxy for the~~  
422 ~~phytoplankton group dinoflagellates (e.g. Meyers, 1997; Castañeda & Schouten, 2011).~~  
423 ~~Cholesterol and cholestanol are produced in a high amounts by zooplankton, although~~  
424 ~~phytoplanktons may also be to a lesser extend a producer, but to a lesser extend (Kohlbach et~~  
425 ~~al., 2021, Taipale et al., 2016, Wittenborn et al., 2020).~~

426

## Brassicasterol

Nevertheless, although brassicasterol is commonly used as biomarker of diatoms, it may be produced by other microalgae (Volkman et al., 1998) not only produced by a specific group of plankton. For example, haptophytes and dinoflagellates produce minor contents of brassicasterol, depending on basic physicochemical parameters like nutrient availability and temperature (Ding et al., 2019). It was noticed (Ding et al., 2019) that brassicasterol contents were higher in diatoms under a balanced N:P supply, whereas dinoflagellates produced more brassicasterol when N:P declined. Consequently, for example, brassicasterol is not a care needs to be taken when using brassicasterol as diatom marker. Nevertheless, brassicasterol is produced by most of the pennate diatoms as major sterol, however, the contents of brassicasterol in radial centric diatoms may, it could vary substantially (Véron et al., 1998). Other phytoplankton groups than diatoms (haptophytes and dinoflagellates), also produce brassicasterol that is dependent on basic physicochemical parameters like nutrient availability and temperature (Ding et al., 2019). It was noticed (Ding et al., 2019) that brassicasterol contents were higher in diatoms under a balanced N:P supply, whereas dinoflagellates produced more of this lipid when N:P declined. However, we do not have enough experimental/field evidence to disapprove that brassicasterol is produced solely by diatoms and hence could be a valid proxy for this group. On the other hand, several studies show that many diatoms produce this sterol brassicasterol in significant amounts, specifically pennates and also many radial centric diatoms (Véron et al., 1998; Ding et al., 2019; Jaramillo-Madrid, et al., 2019, Jaramillo-Madrid, et al., 2020).

Consequently, we are using brassicasterol to indicate the presence of diatoms as a group in the sedimentary organic matter without assigning this lipid biomarker to any specific phylogenetic group, genera, or species to indicate the sources.

### **4.1.12 Physical forcing induced spatial variability in physicochemical properties**

The alkenone-derived SST suggested a cooler northern part (19–21° N) compared to the south along the sampling transect (64° E, Fig. 2d). The annual average of satellite-derived SST also revealed a similar trend. Such variability in SST from north to south could be attributed to monsoon wind variability and related processes. During the summer monsoon, the physicochemical parameters (wind speed, SST, nutrients, mixed layer depths [MLDs]) along 64° E show distinct north-south demarcation due to the presence of the Findlater Jet (Findlater, 1971). In the northern flank of this jet axis, the maximum influence of upwelling is evidenced by the presence of cooler SSTs, high nutrient levels, and shallower MLDs (Silori et al., 2021; Chowdhury et al., 2021; Chowdhury et al., 2024). Along the axis (~15–18° N) of the Jet the highest wind speeds are recorded (Silori et al., 2021; Chowdhury et al., 2021; Chowdhury et al., 2024). The coolest SST value at 15° N is most likely due to the advection of cool nutrient-rich upwelled waters from the western coastal Arabian Sea (Bauer et al., 1991). Furthermore, such high wind speeds for a prolonged period may also lead to evaporative heat loss leading to a decrease in SST. Contrarily, in the south downwelling induced deeper MLDs (>100 m), nutrient-poor waters along with higher SSTs are observed (Latasa and Bidigare, 1998; Chowdhury et al., 2021; Silori et al., 2021). During the winter monsoon, surface circulation reverses in this region, and in the northern Arabian Sea cold dry wind leads to evaporative cooling and subsequent convection leading to cooler SSTs, and high nutrient levels. At the same time, southern regions remain oligotrophic and warm. During the intermonsoon and premonsoon, SST increases and nutrient level reduces substantially along the entire transect

(Prasannakumar and Narvekar, 2005). Consistent with this fact, the annual average satellite-derived Chl<sub>a</sub> values (Fig. 1c) also indicated higher phytoplankton biomass in the north induced by nutrient enrichment, whereas the south was mostly low productive.

## **4.2.23 Spatial variability in particle flux, and phytoplankton dynamics**

### **4.2.23.1 Organic matter**

The northernmost stations were the hotspots for particulate organic matter (POM) flux and sink to the sediment floor (Fig. 2). The positioning of SST in the RDA plot (Fig. 4) opposite TOC, TN, diatom frustules, and phytoplankton lipid biomarkers also supported this fact. The north-south variability in phytodetritus flux could be also influenced by dissolved oxygen levels within the mesopelagic zone (Fig. 5) as it directly controls microbial degradation and zooplankton activity (Moriceau et al., 2018; Iversen, 2023). In our sampling transect, the northern stations are under the influence of intense OMZ-oxygen deficiency which decreases and the-in intensity and as well as the-and thickness reduces while moving towards the -south ward (Banse et al., 2014). In their synthesis, Banse et al. (2014) showed that the median DO values within 150–500 m depth in the northern stations within the core OMZ vary between 0.04 and 0.30 mL L<sup>-1</sup>. Conversely, in the south, these values increased to 0.24–0.72 mL L<sup>-1</sup>. Such spatial variability in OMZ distribution/intensity across the stations could substantially alter the rate of organic matter mineralization, zooplankton abundance (Cavan et al., 2017), and particle flux attenuation (François et al., 2002; Keil et al., 2016). Fast and efficient mineralization within the mesopelagic may allow less organic matter to be transported, whereas partial remineralization may lead to higher organic matter export flux (Ragueneau et al., 2006). Therefore, the northern stations with-at an intense OMZ may have a higher preservation potential of organic matter compared to the south (Fig. 5) as mentioned by Schulte et al. (2000).

### **4.2.3.2.2 Phytoplankton biomarkers Lipid biomarkers as indicators of phytoplankton and zooplankton**

Phytoplankton and zooplankton produce specific lipid biomarkers that are stored in ocean sediments (Castañeda and Schouten, 2011; Meyer 1997; Volkman et al., 1998; Volkman, 2003) and are commonly used to reconstruct past environmental changes (Castañeda and Schouten, 2011; Eglinton and Eglinton, 2008). For instance, calcifying nanophytoplankton *Gephyrocapsa huxleyi* (also known as *Emiliania huxleyi*) and *Gephyrocapsa oceanica* are known to be the main producers of C<sub>37</sub> (C<sub>37:2</sub> and C<sub>37:3</sub>) alkenones in the ocean (Brassell et al., 1986; Eglinton and Eglinton, 2008; Prahl and Wakeham, 1987). In modern and past climate studies C<sub>37:2</sub> and C<sub>37:3</sub> alkenones are used extensively as reliable SST proxies (Prahl et al., 1988; Sonzogni et al., 1997). Among sterols, dinosterol and its degradative product dinostanol are often used as a proxy to represent dinoflagellates (Meyers, 1997; Castañeda and Schouten, 2011).

Brassicasterol a commonly used biomarker of diatoms, may be produced by other microalgae (Volkman et al., 1998). For example, haptophytes and dinoflagellates produce minor contents of brassicasterol, depending on physicochemical parameters like nutrient availability and temperature (Ding et al., 2019). Brassicasterol contents could be higher in diatoms under a balanced N:P supply, whereas a reduced N:P leads to higher brassicasterol production in dinoflagellates (Ding et al., 2019). Nevertheless, brassicasterol is produced by most of the pennate diatoms as major sterol, however, the quantity may vary substantially in radial centric diatoms (Véron et al., 1998). Although we do not have enough experimental/field evidence to disapprove that brassicasterol is produced solely by diatoms and hence could be a valid proxy for this group, several studies show that many diatoms produce brassicasterol in significant

524 [amounts, specifically pennates and also many radial centric diatoms \(Véron et al. 1998; Ding](#)  
525 [et al., 2019; Jaramillo-Madrid, et al., 2019; Jaramillo-Madrid, et al., 2020\). Likewise, we are](#)  
526 [using brassicasterol to indicate the presence of diatoms as a group in the sedimentary organic](#)  
527 [matter without assigning this lipid biomarker to any specific phylogenetic group, genera, or](#)  
528 [species to indicate the sources.](#)

529  
530 TOC-normalized lipid biomarker contents ~~collected from the surface sediment~~  
531 ~~represent~~ indicate the relative contribution of ~~individual major~~ phytoplankton groups to total  
532 organic matter ~~transfer from the upper oceanic layers to the deep sea floor~~ found ~~in surface~~  
533 ~~sediments.~~ In this study, Both total and TOC-normalized phytoplankton lipid biomarkers  
534 revealed that dinoflagellates, diatoms, and coccolithophores were the dominant phytoplankton  
535 groups ~~transferring carbon to the surface sediment~~ (Fig. 2). All studies available from the  
536 Arabian Sea using biomarkers (Schubert et al., 1998; Schulte et al., 1999; 2000; Prahl et al.,  
537 2000) showed that dinosterol contents were higher than brassicasterol, both in sediment core  
538 and trap samples, suggesting greater contributions of dinoflagellates compared to diatoms.  
539 Likewise, we also observed In this study, nearly 1.5 times higher dinosterol contents  
540 compared to brassicasterol ~~all along the transect also confirmed this. Likewise, t~~The dominance  
541 of dinosterol, C<sub>37</sub>-alkenones, and some species-specific ~~biomarkers~~ lipid biomarkers for  
542 diatoms was found in sediment trap samples (2220 m depth) from the ~~Central-central Arabian~~  
543 ~~Sea~~ (Prahl et al., 2000), in two sediment core samples from the northeastern and southern  
544 Arabian Sea (Schulte et al., 1999). Further, a long sediment core from the northern Arabian  
545 Sea close to our sampling locations (22° 29.31' N, 65° 38.9' E) (Schubert et al., 1998) also  
546 reported about the same dominating phytoplankton groups in the Arabian Sea over the past 0.2  
547 million years.

548  
549 ~~In this context, it should be mentioned that attributing any specific sterol contents to a particular~~  
550 ~~phytoplankton group to some extent could be somewhat biased and the contribution of more~~  
551 ~~than one group cannot be overruled. For example, brassicasterol is produced by most of the~~  
552 ~~pennate diatoms, however, for radial centric, it could vary substantially (Véron et al., 1998).~~  
553 ~~Other phytoplankton groups than diatoms (haptophytes and dinoflagellates), also produce~~  
554 ~~brassicasterol that is dependent on basic physicochemical parameters like nutrient availability~~  
555 ~~and temperature (Ding et al., 2019). It was noticed (Ding et al., 2019) that brassicasterol~~  
556 ~~contents were higher in diatoms under a balanced N:P supply, whereas dinoflagellates~~  
557 ~~produced more of this lipid when N:P declined. However, we do not have enough~~  
558 ~~experimental/field evidence to disapprove that brassicasterol is produced by diatoms and hence~~  
559 ~~could be a valid proxy for this group. On the other hand, several studies show many diatoms~~  
560 ~~produce this sterol, specifically pennates and also many radial centric (Véron et al. 1998; Ding~~  
561 ~~et al., 2019; Jaramillo-Madrid, et al., 2019). Here we are using brassicasterol to indicate the~~  
562 ~~presence of diatoms as a group in the sedimentary organic matter without assigning to any~~  
563 ~~phylogenetic group, genera, or species to indicate the sources.~~

564 Since diatoms predominate over dinoflagellates during phytoplankton blooms (Chowdhury et  
565 al., 2021; 2024) a higher contribution of brassicasterol over dinosterol ~~can~~ should be expected,  
566 however, it was the opposite in our study. This reverse trend can be explained by the seasonal  
567 succession of phytoplankton communities in surface layers mostly driven by nutrient  
568 stoichiometry related to monsoon wind forcings and grazing (Prahl et al., 2000; Rixen et al.,  
569 2019a). It should be noted that organic matter on the surface sediment accumulates throughout  
570 the year with variable depositional rates. Monsoon reversal also leads to changes in the  
571 phytoplankton community (Sawant and Madhupratap, 1996; Latasa and Bidigare, 1998) that  
572 may also affect the transfer of phytodetritus to the sea floor. Consequently, diatom frustules

573 largely represent the signature of the most productive ~~periods~~seasons. ~~However~~In contrast, the  
574 nutrient-poor phases are usually dominated by dinoflagellates and other calcifying  
575 nanophytoplankton. Dinoflagellates grow slowly in nutrient-poor warm waters and can remain  
576 there for longer periods (k-strategists) (Smayda and Reynolds, 2001; Glibert et al., 2016).  
577 Likewise, this situation can be ~~compared to~~found at the southern stations, where high SSTs and  
578 oligotrophic conditions were more favorable for the growth of dinoflagellates (Chowdhury et  
579 al., 2021; 2024). This is reflected south of the 15° N station by the occurrences of  
580 dinoflagellates like *Gymnodinium* sp., *Gyrodinium* sp, and *Katodinium* sp. with small cells  
581 (Garrison et al., 1998; Chowdhury et al., 2021).

582 Moreover, unlike diatoms, which are ~~photo~~autotrophs, most dinoflagellates could be either  
583 heterotrophs or mixotrophs (Stoecker, 1999; Stoecker et al., 2017) which actively graze on  
584 smaller phytoplankton including diatoms and even could be detritivorous feeding on particles  
585 (García-Oliva et al., 2022). Mixotrophs could consume prey to meet their cellular nitrogen  
586 demand and can simultaneously perform photosynthesis to gain carbon (Stoecker et al., 2017).  
587 In the Arabian Sea, ~~dissolved inorganic nitrogen is the limiting nutrient and~~ a significant part  
588 of the ~~available dissolved inorganic~~ nitrogen is lost due to strong denitrification within the  
589 OMZ ~~and often becomes the growth-limiting nutrient for phytoplankton~~ (Ward et al., 2006).  
590 Therefore, particularly during the stratified oligotrophic phases like intermonsoon and  
591 premonsoon, when SST increases ~~followed by~~fostering stratification, nanophytoplankton, and  
592 dinoflagellates dominate over diatoms. Hence, the overall contribution of dinoflagellates on an  
593 annual basis could exceed diatoms as dinoflagellates are constantly present during both high-  
594 nutrient regimes and low-nutrient stratified warm water periods.

595 Another possible factor for the observed variability in brassicasterol to dinosterol could be due  
596 to differences in their labile nature. It was claimed that diatom-rich organic matter could be of  
597 higher lability (François et al., 2002) and may possess low transfer potential to the sea floor  
598 (Alonso-González et al., 2010). Contrary to this, it was also observed that compared to other  
599 phytoplankton (Cabrera-Brufau et al., 2021) diatom-rich organic matter is more of a refractory  
600 nature against mesopelagic microbial degradation. Moreover, the phytodetritus of diatom  
601 origin could be preferably ~~eaten~~consumed by the benthic communities than other  
602 phytoplankton groups (Nomaki et al., 2021) and could be one of the reasons for lower  
603 brassicasterol over dinosterol in the surface sediment. This is indeed difficult to conclude as  
604 we do not have enough experimental evidence supporting/contradicting these hypotheses.  
605 Further, as mentioned before we can not exclude, that brassicasterol is sourced by other  
606 phytoplankton groups than diatoms.

607 In the central Arabian Sea, coccolithophores constitute an important part of the  
608 nanophytoplankton community (Andruleit et al., 2004; [Schiebel et al., 2004](#); Mergulhao et al.,  
609 2006). The relatively high occurrences of substantial amounts of C<sub>37</sub>-alkenones all along the  
610 transect in our study indicate that coccolithophores may also contribute as a major part of  
611 sinking phytodetritus, with slightly higher values towards the north (Fig. 2h). Sediment trap  
612 studies from the south of the Findlater Jet (Mergulhao et al., 2006) reported the flux of  
613 coccolithophores throughout the year justifying our observations.

#### 614 **4.2.3-34 Diatom frustules**

615 In our previous study (Pandey et al., 2023), using the topmost (0–0.5 cm) part of the cores, a  
616 trend in diatom frustule abundance and diversity from north to south was observed. –After  
617 compiling the data from 0.5 to 1 cm thea similar trend was noticed.– The highest abundance of  
618 diatom frustules coupled with TOC and TN contents ~~wasere~~ found in the northern stations (~~19–~~  
619 ~~21° N~~), which most likely indicated higher organic matter transfer to the sediment compared

620 to the southern stations. The RDA plot (Fig. 4) also revealed that the abundance of large centric  
621 diatoms like *Coscinodiscus*, *Rhizosolenia*, TOC, and TN contents as well as brassicasterol were  
622 grouped and correlated significantly. In this context, it should be noted that the correlation  
623 between brassicasterol and the major diatom taxa does not necessarily suggest that they are the  
624 sole producers of this lipid biomarker as mentioned in the previous sections. This correlation  
625 most probably indicates that the highest production of brassicasterol and diatom bloom might  
626 have cooccurred and during this period, large diatoms like *Rhizosolenia* or *Coscinodiscus* also  
627 dominated with many other centric and pennate diatoms that produce brassicasterol.

628 During both summer (Chowdhury et al., 2021) and winter monsoons (Sawant and  
629 Madhupratap, 1996) in the northern Arabian Sea, *Coscinodiscus* and *Rhizosolenia* are the  
630 major diatoms forming blooms and consequently, dominate the ~~partiele~~ flux of ~~(opal~~/biogenic  
631 silica) (Rixen et al., 2019a). A higher abundance of large *Rhizosolenia* frustules was also seen  
632 in the sediment trap samples from the central Arabian Sea after the summer monsoon bloom  
633 (Rixen et al., 2019a). The contribution of heavily silicified diatom frustules may in addition  
634 provide ballasting effects (Smetacek, 1985; Tréguer et al., 2018) facilitating efficient organic  
635 matter export compared to other phytoplankton groups (Buesseler, 1998; Boyd and Newton,  
636 1999; Zúñiga et al., 2021). Diatom bloom development in the Arabian Sea was found to be  
637 associated with dissolved silica (DSi) availability (Chowdhury et al., 2021) and the depth of  
638 the silicicline (Anju et al., 2020). The northern stations become DSi depleted (<2 µM) at the  
639 end of the bloom (Chowdhury et al., 2021) and may lead to a mass sinking of frustules  
640 (Smetacek, 1985; Krause et al., 2019) or they can be grazed and cell death may also occur due  
641 to viral attacks (Agusti and Duarte, 2000). On the other hand, the abundance of small chain-  
642 forming diatoms such as *Thalassiosira*, *Pseudo-nitzschia*, *Nitzschia*, and *Thalassionema*,  
643 enhanced in the surface sediment in the southern stations (Fig. 3). ~~Low~~ nutrient conditions  
644 prevail in this region even during summer and winter monsoons. During the intermonsoon and  
645 premonsoon oligotrophy intensifies in these regions supporting the growth of smaller diatoms  
646 or non-diatoms (Garrison et al., 1998; Tarran et al., 1999; Chowdhury et al., 2021) that could  
647 sink slower compared to the larger cells in the north (Buesseler and Boyd, 2009).

648 Moreover, diatom frustules may dissolve while sinking and some of them (e. g. usually, the  
649 thickly silicified frustules) reach the abyssal plain and can be well are preserved in the seafloor  
650 sediments—floor. Nevertheless, the organic coating that protects siliceous frustules from  
651 dissolution (Lewin, 1961), can be degraded by heterotrophic bacterial activity (Bidle and  
652 Azam, 1999; Roubéix et al., 2008). The presence of OMZ in the northern stations (200–1200  
653 m) could therefore slow down such dissolution facilitating frustules to reach the sea floor. On  
654 the other hand, in the south, small and thinly silicified diatom frustules (mostly due to DSi  
655 limitation) may be more fragile as they travel through the well-oxygenated water column and  
656 higher heterotrophic activity may enhance the risk of dissolution—degradation leading to  
657 reduced frustules abundance on the seabed. In addition to this, the almost 700 m deeper water  
658 column in the south compared to the north could enhance the scope of degradation of sinking  
659 particles. This is consistent with our observation.

#### 660 **4.2.4 ~~45~~ Zooplankton grazing**

661  
662 Two proxies representing zooplankton have been considered in this study 1) sterol biomarkers  
663 [cholesterol (Fig. 2i), and its degradative product cholestanol (Fig. 2j)], and 2) radiolarians  
664 (Fig. 2k). Cholesterol and cholestanol are produced in high amounts by zooplankton and are  
665 used as zooplankton proxies, nevertheless, some phytoplankton may also produce them in  
666 insignificant quantities (Kohlbach et al., 2021; Taipale et al., 2016; Wittenborn et al., 2020).  
667 Accordingly, ~~the~~ the highest concentration of TOC-normalized cholesterol was found in the south  
668 indicating more zooplankton activity. In the RDA biplot, SST was ~~elubbed~~ grouped with

669 cholestanol and was on the same side ~~of as~~ cholesterol indicating higher zooplankton activity  
670 in the south. The association of TIC with cholesterol indicates that calcareous zooplankton  
671 could also be a source of cholesterol. Consequently, a higher fecal matter production could  
672 enhance particle flux compared to the north. Nonetheless, a major part of the fecal matter could  
673 also be degraded within the upper mesopelagic layer as reported by Iversen et al. (2017). In the  
674 Southern Ocean, The authors observed that mmore than 87% of fecal matter produced in the  
675 surface ocean can be lost via remineralization before reaching the upper mesopelagic zones  
676 (300 m) ~~in the Southern Ocean~~(Iversen et al. 2017). Likewise, the warmer temperature in the  
677 mesopelagic water column at of our sampling study—locations could facilitate faster  
678 mineralization. Zooplankton grazing could largely alter the magnitude of carbon export flux  
679 (Moriceau et al., 2018). Thus, the low abundance of mesozooplankton within the OMZ may  
680 decrease defragmentation, which in turn slows down the bacterial remineralization of  
681 phytodetritus allowing a higher amount of carbon to be exported to the abyssal plain (Cavan et  
682 al., 2017) (Fig. 5). Likewise, the lower zooplankton activity in the mesopelagic ~~within the~~OMZ  
683 of the Arabian Sea (Wishner et al., 1998) may hinder particle fragmentation that usually  
684 accelerates degradation (Briggs et al., 2020). Likewise Similarly, at the northern stations, lower  
685 zooplankton abundance within the OMZ (Cavan et al., 2017) may restrict particle flux  
686 attenuation (Fig. 5).

687 In the western and central Arabian Sea, nearly 50–100% of the diatom population can be grazed  
688 by copepods (Landry et al., 1998; Smith et al., 1998; Gauns et al., 2005). Importantly, diatom  
689 cell size can be a crucial factor that determines their grazing rates. Copepods exhibit the highest  
690 grazing rate when the ratio between prey and predator body size remains 18:1 on average  
691 (Hansen et al., 1994). In the north and at the axis of the Findlater Jet, the higher availability of  
692 nutrients, particularly DSi could promote large and thickly silicified diatoms which are difficult  
693 to graze for copepods (Hansen et al., 1994; Ryderheim et al., 2022). Subsequently, large centric  
694 diatoms like *Coscinodiscus radiatus* and *Rhizosolenia* spp. could escape grazing by copepods  
695 (Jansen, 2008; Löder et al., 2011) and can sink to the seafloor sediment floor (Buesseler and  
696 Boyd, 2009; Kemp et al., 2006). On the contrary, the bloom-forming diatoms with thinly  
697 silicified frustules like *Chaetoceros* and *Leptocylindrus* (Sawant and Madhupratap, 1996;  
698 Chowdhury et al., 2021) can be grazed easily and are usually not found in the sediment.  
699 However, the organic signature lipid biomarkers of these diatoms (brassicasterol) may be  
700 preserved after transport through the water column in faecal pellets ~~can be reflected in surface~~  
701 sediments. sary biomarkers like brassicasterol. In ~~the the~~ case of the southern stations, smaller  
702 diatoms or non-diatoms could be consumed by microzooplankton (Swanberg and Anderson,  
703 1985). Corroborating with this fact, the significantly higher number of radiolarians (Fig. 2k)  
704 which mostly consume smaller phytoplankton, bacterioplankton, and copepods (Caron et al.,  
705 1995) were higher in the south. A high abundance of radiolarians dominated by *Tetrapyle* sp.  
706 that are found under high salinity was also reported by a previous study from the Arabian Sea  
707 (Gupta, 2003).

#### 708 709 **4.23.5.6 Influence of lateral advection**

710  
711 Since there is evidence of advected waters reaching from the western Arabian Sea to its central  
712 part, the chances of particle transport also need to be considered. Stable Nnitrogen-stable  
713 isotopic values of particulate organic matter ( $\delta^{15}\text{N}_{\text{POM}}$ , Silori et al., 2021) revealed that nutrient  
714 enrichment mostly takes place via advection from the upwelling system as well as entrainment  
715 close to the axis of the Findlater Jet (16–18° N). Earlier studies also noticed the presence of  
716 slightly low saline waters in this region probably due to advection from the western Arabian  
717 Sea (Prasanna Kumar et al., 2000). Additionally, Silori et al. (2021) reported lower  $\delta^{15}\text{N}$  values

718 of particulate nitrogen during summer monsoon at the stations influenced by the axis  
719 suggesting laterally advected dissolved inorganic nitrogen from the Somali upwelling region.  
720 However, so far there is no report claiming that particulate organic matter can be advected such  
721 a long distance (~600 km) without being grazed/remineralized/sinking. Contrarily, there is  
722 plenty of evidence showing a direct relation between phytoplankton bloom and particle flux in  
723 these regions (Haake et al., 1993; Rixen et al., 2019a). Thus, the possibility of lateral transport  
724 of phytoplankton or detritus from the western Arabian Sea to the seabed of the central Arabian  
725 Sea may be ~~partly overruled~~ overlain by vertical particle flux.

726

## 727 **Conclusions**

728 In our previous study (Pandey et al., 2023) using diatom frustules and sedimentary bulk  
729 parameters from the topmost part of the sediment core (0–0.5 cm), we established a link  
730 between the spatial trend in organic matter variability, atmospheric forcing, and phytoplankton  
731 bloom. The ~~presentis~~ study aims for the first time to elucidate phytoplankton-driven particle  
732 flux to the sea-floor using sedimentary ~~organic-lipid~~ biomarkers from the central Arabian Sea.  
733 Such studies linking sedimentary organic matter to physical forcings and phytoplankton  
734 community have rarely been ~~studied-conducted~~ in the central Arabian Sea. Importantly, most  
735 of the studies using sediment traps focused on diatoms and coccolithophores, but neglected  
736 dinoflagellates (Nair et al., 1989). A few studies proposed that the diatom blooms could be  
737 replaced by dinoflagellates. On the other hand, -another study (Schubert et al., 1998), revealed  
738 that the relative contribution of dinosterol was higher than brassicasterol over the last 0.2  
739 million years in this basin. Following this concept, we crosschecked the organic matter from  
740 the top 1 cm of surface sediments from more locations across a spatially variable transect (from  
741 high to low productive).

742 Our results ~~also~~ indicated that dinoflagellates have contributed more to the sedimentary  
743 phytodetritus compared to diatoms even in the recent past. We propose that diatoms and  
744 coccolithophores do contribute to sedimentary particle flux. However, the dinoflagellates  
745 dominate due to their ~~smart~~ survival strategies during poor nutrient supply. We show that the  
746 distinct spatial variability in physical forcing drives the phytoplankton bloom and the particle  
747 flux is also closely coupled ~~with this fact~~. Nevertheless, we also need to mention that the diatom  
748 community constructed from the frustules is not the direct producer of brassicasterol; the  
749 community provides more information about the surface oceanic processes including nutrient  
750 availability. The northernmost station in the central Arabian Sea was found to be a hotspot for  
751 sinking particles followed by subsequent preservation mostly due to the prevailing OMZ (Fig.  
752 5). Both summer and winter monsoon-induced phytoplankton bloom dominated by diatoms led  
753 to the sinking of large thickly silicified frustules on the sediment floor. We hypothesized that  
754 the low oxygen within the thick OMZ could slow down the dissolution of frustules as well as  
755 heterotrophic degradation and fragmentation by zooplankton leading to low flux attenuation.  
756 Contrarily, in the south, higher dissolved oxygen levels could facilitate faster remineralization  
757 and higher zooplankton activity resulting in more flux attenuation and reduced particle  
758 transport to the sea floor. Contrary to the global scenario of expanding OMZs, a few recent  
759 ~~modeling~~ studies (Vallivattathillam et al., 2023; Liu et al., 2024) showed that the southern  
760 part of the OMZ can get thinner in the future due to the higher supply of oxygen. Such changes  
761 could facilitate higher heterotrophic activities within the mesopelagic and thus could impact  
762 particle flux attenuation in this region and need to be investigated.

## 763 **Acknowledgments**

764 MP was supported by the Department of Science and Technology (DST) - Inspire Fellowship.  
765 This study is an outcome of the CSIR-NIO in-house program “Impact of Climate Change on



766 the Physics, Biogeochemistry, and the Ecology of the North Indian Ocean (CliCNIO)” (MLP  
767 1802) funded by the Council of Scientific and Industrial Research (CSIR). We express our  
768 gratitude to the captain, scientists, technical staff, ship cell staff, deckhands, and the students  
769 onboard *RV Sindhu Sadhana* (SSD 068) for their constant help and support during the cruise.  
770 We are thankful to the Director, CSIR NIO for his kind support. Ms. Teja Naik is acknowledged  
771 for ~~their~~her technical help in using the Coulometer under the central analytical facility in CSIR,  
772 NIO, Goa. The contribution number is XXXX. NB was funded by the Deutsche  
773 Forschungsgemeinschaft (DFG, German Research Foundation) under Germany’s Excellence  
774 Strategy – EXC 2037 'CLICCS - Climate, Climatic Change, and Society' – Project Number:  
775 390683824, contribution to the Center for Earth System Research and Sustainability (CEN) of  
776 Universität Hamburg. ~~The author(s) wish to acknowledge use of the Ferret program for analysis  
777 and graphics in this paper. Ferret is a product of NOAA's Pacific Marine Environmental  
778 Laboratory. (Information is available at <http://ferret.pmel.noaa.gov/Ferret/>).~~

779  
780 **Availability of data and materials:** [The data are available online at Mendeley Data \(DOI:  
781 10.17632/xm4nxzdx2.1\)](https://doi.org/10.17632/xm4nxzdx2.1)

## 782 **Statements and Declarations**

783 **Competing Interests:** *The authors have no relevant financial or non-financial interests to  
784 disclose.*

785 **Ethical Approval: Not applicable**

786 **Consent to Participate: Not applicable**

787 **Consent to Publish: Not applicable**

788 **Authors' Contributions:** *MP: Conceptualization, sampling, sample analysis; formal  
789 analysis, data curation, writing original manuscript and editing; HB: Conceptualization; Fund  
790 acquisition; sampling; manuscript reviewing and editing; DB: sampling; manuscript  
791 reviewing and editing NB: Sample analysis, Conceptualization; manuscript reviewing and  
792 editing BG: Conceptualization; reviewing and editing*

## 793 **References**

- 794 1. Abrantes, F.F.G. and Sancetta, C.: Diatom assemblages in surface sediments reflect  
795 coastal upwelling off southern Portugal, *Oceanologica acta*, 8,7–12, 1985.
- 796 2. Agustí, S. and Duarte, C.M.: Strong seasonality in phytoplankton cell lysis in the NW  
797 Mediterranean littoral, *Limnology and Oceanography*, 45, 940–947,  
798 <https://doi.org/10.4319/lo.2000.45.4.0940>, 2000.
- 799 3. Alonso-González, I.J., Arístegui, J., Lee, C., Sanchez-Vidal, A., Calafat, A., Fabrés, J.,  
800 Sangrá, P., Masqué, P., Hernández-Guerra, A. and Benítez-Barrios, V.: Role of slowly  
801 settling particles in the ocean carbon cycle, *Geophysical research letters*, 37,  
802 <https://doi.org/10.1029/2010GL043827>, 2010.
- 803 4. Andruleit, H., Rogalla, U. and Stäger, S.: From living communities to fossil  
804 assemblages: origin and fate of coccolithophores in the northern Arabian Sea,  
805 *Micropaleontology*, 50, 5-21, [https://doi.org/10.2113/50.Suppl\\_1.5](https://doi.org/10.2113/50.Suppl_1.5), 2004.
- 806 5. Anju, M., Sreeush, M.G., Valsala, V., Smitha, B.R., Hamza, F., Bharathi, G. and Naidu,  
807 C.V.: Understanding the role of nutrient limitation on plankton biomass over Arabian  
808 Sea via 1-D coupled biogeochemical model and bio-Argo observations, *Journal of  
809 Geophysical Research: Oceans*, 125, e2019JC015502,  
810 <https://doi.org/10.1029/2019JC015502>, 2020.

- 811 6. Armbrrecht, L.H., Lowe, V., Escutia, C., Iwai, M., McKay, R. and Armand, L.K.:  
812 Variability in diatom and silicoflagellate assemblages during mid-Pliocene glacial-  
813 interglacial cycles determined in Hole U1361A of IODP Expedition 318, Antarctic  
814 Wilkes Land Margin, Marine Micropaleontology, 139, 28–41,  
815 <https://doi.org/10.1016/j.marmicro.2017.10.008>, 2018.
- 816 7. Banse, K.: Seasonality of phytoplankton chlorophyll in the central and northern  
817 Arabian Sea, Deep Sea Research Part A, Oceanographic Research Papers, 34, 713–723,  
818 [https://doi.org/10.1016/0198-0149\(87\)90032-X](https://doi.org/10.1016/0198-0149(87)90032-X), 1987.
- 819 8. Banse, K., Naqvi, S.W.A., Narvekar, P.V., Postel, J.R. and Jayakumar, D.A.: Oxygen  
820 minimum zone of the open Arabian Sea: variability of oxygen and nitrite from daily to  
821 decadal timescales, Biogeosciences, 11, 2237–2261, [https://doi.org/10.5194/bg-11-](https://doi.org/10.5194/bg-11-2237-2014)  
822 [2237-2014](https://doi.org/10.5194/bg-11-2237-2014), 2014.
- 823 9. Barnett, P.R.O., Watson, J. and Connelly, D.: A multiple corer for taking virtually  
824 undisturbed samples from shelf, bathyal and abyssal sediments, Oceanologica acta, 7,  
825 399–408, 1984.
- 826 10. Bauer, S., Hitchcock, G.L., Olson, D.B.: Influence of monsoonally-forced Ekman  
827 dynamics upon surface layer depth and plankton biomass distribution in the Arabian  
828 Sea, Deep Sea Research, Part A Oceanographic Research Papers 38, 531–553,  
829 [https://doi.org/10.1016/0198-0149\(91\)90062-K](https://doi.org/10.1016/0198-0149(91)90062-K), 1991.
- 830 11. Behrenfeld, M.J., O'Malley, R.T., Siegel, D.A., McClain, C.R., Sarmiento, J.L.,  
831 Feldman, G.C., Milligan, A.J., Falkowski, P.G., Letelier, R.M. and Boss, E.S.: Climate-  
832 driven trends in contemporary ocean productivity, Nature, 444, 752–755,  
833 <https://doi.org/10.1038/nature05317>, 2006.
- 834 12. Bhattathiri, P.M.A., Pant, A., Sawant, S., Gauns, M., Matondkar, S.G.P. and  
835 Mohanraju, R.: Phytoplankton production and chlorophyll, Current Science, 71, 1996.
- 836 13. Bidle, K.D. and Azam, F.: Accelerated dissolution of diatom silica by marine bacterial  
837 assemblages, Nature, 397, 508–512, <https://doi.org/10.1038/17351>, 1999.
- 838 14. Boyd, P.W. and Newton, P.P.: Does planktonic community structure determine  
839 downward particulate organic carbon flux in different oceanic provinces?, Deep Sea  
840 Research Part I: Oceanographic Research Papers, 46, 63–91,  
841 [https://doi.org/10.1016/S09670637\(98\)00066-1](https://doi.org/10.1016/S09670637(98)00066-1), 1999.
- 842 14.15. [Brassell, S.C., Brereton, R.G., Eglinton, G., Grimalt, J., Liebezeit, G., Marlowe,](https://doi.org/10.1016/S0146-6380(86)80001-8)  
843 [I.T., Pflaumann, U. and Sarnthein, M.: Palaeoclimatic signals recognized by](https://doi.org/10.1016/S0146-6380(86)80001-8)  
844 [chemometric treatment of molecular stratigraphic data, Organic Geochemistry, 10\(4-](https://doi.org/10.1016/S0146-6380(86)80001-8)  
845 [6\), 649–660, https://doi.org/10.1016/S0146-6380\(86\)80001-8, 1986.](https://doi.org/10.1016/S0146-6380(86)80001-8)
- 846 15.16. [Briggs, N., Dall'Olmo, G. and Claustre, H.: Major role of particle fragmentation](https://doi.org/10.1126/science.aay1790)  
847 [in regulating biological sequestration of CO<sub>2</sub> by the oceans, Science, 367, 791–793,](https://doi.org/10.1126/science.aay1790)  
848 <https://doi.org/10.1126/science.aay1790>, 2020.
- 849 16.17. [Buesseler, K.O. and Boyd, P.W.: Shedding light on processes that control](https://doi.org/10.4319/lo.2009.54.4.1210)  
850 [particle export and flux attenuation in the twilight zone of the open ocean, Limnology](https://doi.org/10.4319/lo.2009.54.4.1210)  
851 [and Oceanography, 54, 1210–1232, https://doi.org/10.4319/lo.2009.54.4.1210](https://doi.org/10.4319/lo.2009.54.4.1210), 2009.
- 852 17.18. [Buesseler, K.O.: The decoupling of production and particulate export in the](https://doi.org/10.1029/97GB03366)  
853 [surface ocean, Global Biogeochemical Cycles, 12, 297–310,](https://doi.org/10.1029/97GB03366)  
854 <https://doi.org/10.1029/97GB03366>, 1998.
- 855 18.19. [Cabrera-Brufau, M., Arin, L., Sala, M.M., Cermeño, P. and Marrasé, C.: Diatom](https://doi.org/10.3389/fmars.2021.683354)  
856 [dominance enhances resistance of phytoplanktonic POM to mesopelagic microbial](https://doi.org/10.3389/fmars.2021.683354)  
857 [decomposition, Frontiers in Marine Science, 8, p.683354,](https://doi.org/10.3389/fmars.2021.683354)  
858 <https://doi.org/10.3389/fmars.2021.683354>, 2021.
- 859 20. Caron, D.A., Michaels, A.F., Swanberg, N.R. and Howse, F.A.: Primary productivity  
860 by symbiont-bearing planktonic sarcodines (Acantharia, Radiolaria, Foraminifera) in

861 surface waters near Bermuda, *Journal of Plankton Research*, 17, 103–129.  
862 <https://doi.org/10.1093/plankt/17.1.103>, 1995.

863 ~~19-21.~~ Castañeda, I.S. and Schouten, S., ~~2011.~~: [A review of molecular organic proxies](https://doi.org/10.1016/j.quascirev.2011.07.009)  
864 [for examining modern and ancient lacustrine environments.](https://doi.org/10.1016/j.quascirev.2011.07.009), *Quaternary Science*  
865 *Reviews*, 30(21-22), pp.2851–289, <https://doi.org/10.1016/j.quascirev.2011.07.009>,  
866 2011.

867 ~~20-22.~~ Cavan, E.L., Trimmer, M., Shelley, F. and Sanders, R.: Remineralization of  
868 particulate organic carbon in an ocean oxygen minimum zone. *Nature*  
869 *Communications*, 8(1), p.14847, <https://doi.org/10.1038/ncomms14847>, 2017.

870 ~~21-23.~~ Chowdhury, M., Biswas, H., Mitra, A., Silori, S., Sharma, D., Bandyopadhyay,  
871 D., Shaik, A.U.R., Fernandes, V. and Narvekar, J.: Southwest monsoon-driven changes  
872 in the phytoplankton community structure in the central Arabian Sea (2017–2018):  
873 After two decades of JGOFS, *Progress in Oceanography*, 197, p.102654,  
874 <https://doi.org/10.1016/j.pocean.2021.102654>, 2021.

875 ~~22-24.~~ Chowdhury, M., Biswas, H., Silori, S. and Sharma, D.: Spatiotemporal  
876 variability in phytoplankton size class modulated by summer monsoon wind forcing in  
877 the central Arabian Sea, *Journal of Geophysical Research: Oceans*, 129,  
878 e2023JC019880, <https://doi.org/10.1029/2023JC019880>, 2024.

879 ~~23-25.~~ Copernicus Climate Change Service (C3S), ERA5: Fifth generation of ECMWF  
880 atmospheric reanalyses of the global climate, Copernicus Climate Change Service  
881 Climate Data Store (CDS), 2017.

882 ~~26.~~ Desikachary, T.V.: *Atlas of Diatoms (Marine Diatoms of the Indian Ocean Region)*, 6,  
883 Madras Science Foundation, Madras Fasc, 1–13, 1989.

884 ~~27.~~ Ding, Y., Bi, R., Sachs, J., Chen, X., Zhang, H., Li, L. and Zhao, M., [Lipid biomarker](https://doi.org/10.1016/j.orggeochem.2019.01.008)  
885 [production by marine phytoplankton under different nutrient and temperature regimes.](https://doi.org/10.1016/j.orggeochem.2019.01.008)  
886 *Organic Geochemistry*, 131, 34-49. <https://doi.org/10.1016/j.orggeochem.2019.01.008>,  
887 2019.

888 ~~24-28.~~ Eglinton, T.I. and Eglinton, G., 2008. [Molecular proxies for paleoclimatology,](https://doi.org/10.1016/j.epsl.2008.07.012)  
889 [Earth and Planetary Science Letters](https://doi.org/10.1016/j.epsl.2008.07.012), 275(1–2), 1–16,  
890 <https://doi.org/10.1016/j.epsl.2008.07.012>, 2008.

891 ~~25-29.~~ Engel, A., Wagner, H., Le Moigne, F.A. and Wilson, S.T.: Particle export fluxes  
892 to the oxygen minimum zone of the eastern tropical North  
893 Atlantic, *Biogeosciences*, 14,1825-1838, <https://doi.org/10.5194/bg-14-1825-2017>,  
894 2017.

895 ~~26-30.~~ Field, C.B., Behrenfeld, M.J., Randerson, J.T. and Falkowski, P.: Primary  
896 production of the biosphere: integrating terrestrial and oceanic  
897 components, *Science*, 281, 237–240, <https://doi.org/10.1126/science.281.5374.237>,  
898 1998.

899 ~~27-31.~~ Findlater, J.: Mean monthly airflow at low levels over the western Indian  
900 Ocean (No. 116). HM Stationery Office, Pure Appl. Geophys. PAGEOPH 115, 1251–  
901 1262, <https://doi.org/10.1007/BF00874408>, 1971.

902 ~~28-32.~~ Francois, R., Honjo, S., Krishfield, R. and Manganini, S.: Factors controlling  
903 the flux of organic carbon to the bathypelagic zone of the ocean, *Global*  
904 *Biogeochemical Cycles*, 16, 34–1, <https://doi.org/10.1029/2001GB001722>, 2002.

905 ~~29-33.~~ García-Oliva, O., Hantzsche, F.M., Boersma, M. and Wirtz, K.W.:  
906 Phytoplankton and particle size spectra indicate intense mixotrophic dinoflagellates  
907 grazing from summer to winter. *Journal of Plankton Research*, 44, 224–240,  
908 <https://doi.org/10.1093/plankt/fbac013>, 2022.

909 ~~30-34.~~ Garrison, D.L., Gowing, M.M. and Hughes, M.P.: Nano-and microplankton in  
910 the northern Arabian Sea during the Southwest Monsoon, August–September 1995 A

911 US–JGOFS study, Deep Sea Research Part II: Topical Studies in Oceanography, 45,  
912 2269–2299, [https://doi.org/10.1016/S0967-0645\(98\)00071-X](https://doi.org/10.1016/S0967-0645(98)00071-X), 1998.

913 [31-35.](#) Gauns, M., Madhupratap, M., Ramaiah, N., Jyothibabu, R., Fernandes, V., Paul,  
914 J.T. and Kumar, S.P.: Comparative accounts of biological productivity characteristics  
915 and estimates of carbon fluxes in the Arabian Sea and the Bay of Bengal. Deep Sea  
916 Research Part II: Topical Studies in Oceanography, 52, 2003–2017,  
917 <https://doi.org/10.1016/j.dsr2.2005.05.009>, 2005.

918 [32-36.](#) Glibert, P.M., Wilkerson, F.P., Dugdale, R.C., Raven, J.A., Dupont, C.L.,  
919 Leavitt, P.R., Parker, A.E., Burkholder, J.M. and Kana, T.M.: Pluses and minuses of  
920 ammonium and nitrate uptake and assimilation by phytoplankton and implications for  
921 productivity and community composition, with emphasis on nitrogen-enriched  
922 conditions, Limnology and Oceanography, 61, 165–197,  
923 <https://doi.org/10.1002/lno.10203>, 2016.

924 [33-37.](#) Gupta, S.M.: Orbital frequencies in radiolarian assemblages of the central  
925 Indian Ocean: implications on the Indian summer monsoon, Palaeogeography,  
926 Palaeoclimatology, Palaeoecology, 197(1-2), 97–112, [https://doi.org/10.1016/S0031-0182\(03\)00388-2](https://doi.org/10.1016/S0031-0182(03)00388-2), 2003.

928 [34-38.](#) Haake, B., Ittekkot, V., Rixen, T., Ramaswamy, V., Nair, R.R. and Curry, W.B.:  
929 Seasonality and interannual variability of particle fluxes to the deep Arabian Sea, Deep  
930 Sea Research Part I: Oceanographic Research Papers, 40(7), 1323–1344,  
931 [https://doi.org/10.1016/0967-0637\(93\)90114-I](https://doi.org/10.1016/0967-0637(93)90114-I), 1993.

932 [35-39.](#) Hansen, B., Bjornsen, P.K. and Hansen, P.J.: The size ratio between planktonic  
933 predators and their prey, Limnology and oceanography, 39(2), 395–403,  
934 <https://doi.org/10.4319/lo.1994.39.2.0395>, 1994.

935 [36-40.](#) Hu, L., Liu, Y., Xiao, X., Gong, X., Zou, J., Bai, Y., Gorbarenko, S., Fahl, K.,  
936 Stein, R. and Shi, X.: Sedimentary records of bulk organic matter and lipid biomarkers  
937 in the Bering Sea: A centennial perspective of sea-ice variability and phytoplankton  
938 community, Marine Geology, 429, 106308,  
939 <https://doi.org/10.1016/j.margeo.2020.106308>, 2020.

940 [37-41.](#) Iversen, M.H., Pakhomov, E.A., Hunt, B.P., Van der Jagt, H., Wolf-Gladrow,  
941 D. and Klaas, C.: Sinkers or floaters? Contribution from salp pellets to the export flux  
942 during a large bloom event in the Southern Ocean, Deep Sea Research Part II: Topical  
943 Studies in Oceanography, 138, 116–125, <https://doi.org/10.1016/j.dsr2.2016.12.004>,  
944 2017.

945 [42.](#) Iversen, M.H.: Carbon Export in the Ocean: A Biologist's Perspective, Annual Review  
946 of Marine Science, 15, 357–381, [10.1146/annurev-marine-032122-035153](https://doi.org/10.1146/annurev-marine-032122-035153), 2023.

947 [43.](#) Jaramillo-Madrid, A.C., Ashworth, J., Fabris, M. and Ralph, P.J., [Phytosterol](#)  
948 [biosynthesis and production by diatoms \(Bacillariophyceae\). Phytochemistry, 163.46-](#)  
949 [57. https://doi.org/10.1016/j.phytochem.2019.03.018, 2019.](#)

950 [38-44.](#) Jaramillo-Madrid A.C., Ashworth, J., Ralph, P. J., [Levels of Diatom Minor](#)  
951 [Sterols Respond to Changes in Temperature and Salinity. Journal of Marine Science](#)  
952 [and Engineering. 8\(2\), 85, https://doi.org/10.3390/jmse8020085, 2020.](#)

953 [45.](#) Jansen, S.: Copepods grazing on *Coscinodiscus wailesii*: a question of size?, Helgoland  
954 Marine Research, 62(3), 251–255, <https://doi.org/10.1007/s10152-008-0113-z>, 2008.

955 [39-46.](#) [Kohlbach, D., Hop, H., Wold, A., Schmidt, K., Smik, L., Belt, S. T., Keck, Al-](#)  
956 [Hababbeh, A., Woll, M, Graeve, M., Dąbrowska, A. M,s Tatarek, A., Atkinson, A., and](#)  
957 [Assmy, P.: Multiple Trophic Markers Trace Dietary Carbon Sources in Barents Sea](#)  
958 [Zooplankton During Late Summer. Front. Mar. Sci. 7:610248. doi:](#)  
959 [10.3389/fmars.2020.610248, 2021.](#)

960 [40-47.](#) Keil, R.G., Neibauer, J.A., Biladeau, C., van der Elst, K. and Devol, A.H.: A  
961 multiproxy approach to understanding the "enhanced" flux of organic matter through

962 the oxygen-deficient waters of the Arabian Sea, *Biogeosciences*, 13(7), 2077–2092,  
963 <https://doi.org/10.5194/bg-13-2077-2016>, 2016.

964 41.48. Kemp, A.E., Pearce, R.B., Grigorov, I., Rance, J., Lange, C.B., Quilty, P. and  
965 Salter, I., Production of giant marine diatoms and their export at oceanic frontal zones:  
966 Implications for Si and C flux from stratified oceans, *Global Biogeochemical*  
967 *Cycles*, 20(4), <https://doi.org/10.1029/2006GB002698>, 2006.

968 42.49. Krause, J.W., Schulz, I.K., Rowe, K.A., Dobbins, W., Winding, M.H., Sejr,  
969 M.K., Duarte, C.M. and Agustí, S.: Silicic acid limitation drives bloom termination and  
970 potential carbon sequestration in an Arctic bloom, *Scientific Reports*, 9(1), 8149,  
971 <https://doi.org/10.1038/s41598-019-44587-4>, 2019.

972 43.50. Landry, M.R., Brown, S.L., Campbell, L., Constantinou, J. and Liu, H.: Spatial  
973 patterns in phytoplankton growth and microzooplankton grazing in the Arabian Sea  
974 during monsoon forcing, *Deep Sea Research Part II: Topical Studies in Oceanography*,  
975 45(10–11), 2353–2368, [https://doi.org/10.1016/S0967-0645\(98\)00074-5](https://doi.org/10.1016/S0967-0645(98)00074-5), 1998.

976 44.51. Latasa, M. and Bidigare, R.R.: A comparison of phytoplankton populations of  
977 the Arabian Sea during the Spring Intermonsoon and Southwest Monsoon of 1995 as  
978 described by HPLC-analyzed pigments, *Deep Sea Research Part II: Topical Studies in*  
979 *Oceanography*, 45(10-11), 2133–2170, [https://doi.org/10.1016/S0967-0645\(98\)00066-](https://doi.org/10.1016/S0967-0645(98)00066-6)  
980 [6](https://doi.org/10.1016/S0967-0645(98)00066-6), 1998.

981 45.52. Le Moigne, F.A.: Pathways of organic carbon downward transport by the  
982 oceanic biological carbon pump, *Frontiers in Marine Science*, 6, 634,  
983 <https://doi.org/10.3389/fmars.2019.00634>, 2019.

984 46.53. Lewin, J.C.: The dissolution of silica from diatom walls, *Geochimica et*  
985 *Cosmochimica Acta*, 21(3-4), 182–198, [https://doi.org/10.1016/S0016-](https://doi.org/10.1016/S0016-7037(61)80054-9)  
986 [7037\(61\)80054-9](https://doi.org/10.1016/S0016-7037(61)80054-9), 1961.

987 54. Liu, D., Shen, X., Di, B., Shi, Y., Keesing, J.K., Wang, Y. and Wang, Y.:  
988 Palaeoecological analysis of phytoplankton regime shifts in response to coastal  
989 eutrophication, *Marine Ecology Progress Series*, 475, 1–14,  
990 <https://doi.org/10.3354/meps10234>, 2013.

991 47.55. Liu, T., Qiu, Y., Lin, X., Ni, X., Wang, L., Li, H. and Jing, C., *Dissolved oxygen*  
992 *recovery in the oxygen minimum zone of the Arabian Sea in recent decade as observed*  
993 *by BGC-argo floats. Geophysical Research Letters*, 51(12), p.e2024GL108841.  
994 <https://doi.org/10.1029/2024GL108841>, 2024

995 48.56. Löder, M.G., Meunier, C., Wiltshire, K.H., Boersma, M. and Aberle, N.: The  
996 role of ciliates, heterotrophic dinoflagellates and copepods in structuring spring  
997 plankton communities at Helgoland Roads, North Sea, *Marine biology*, 158, 1551–  
998 1580, <https://doi.org/10.1007/s00227-011-1670-2>, 2011.

999 49.57. Madhupratap, M., Kumar, S.P., Bhattathiri, P.M.A., Kumar, M.D.,  
1000 Raghukumar, S., Nair, K.K.C. and Ramaiah, N.: Mechanism of the biological response  
1001 to winter cooling in the northeastern Arabian Sea, *Nature*, 384(6609), 549–552,  
1002 <https://doi.org/10.1038/384549a0>, 1996.

1003 50.58. Marsay, C.M., Sanders, R.J., Henson, S.A., Pabortsava, K., Achterberg, E.P.  
1004 and Lampitt, R.S.: Attenuation of sinking particulate organic carbon flux through the  
1005 mesopelagic ocean, *Proceedings of the National Academy of Sciences*, 112(4), 1089–  
1006 1094, <https://doi.org/10.1073/pnas.141531111>, 2015.

1007 51.59. McCreary, J.P., Murtugudde, R., Vialard, J., Vinayachandran, P.N., Wiggert,  
1008 J.D., Hood, R.R., Shankar, D. and Shetye, S.: Biophysical processes in the Indian  
1009 Ocean, *Indian Ocean biogeochemical processes and ecological variability*, 185, 9–32,  
1010 <https://doi.org/10.1029/2008GM000768>, 2009.

- 1011 [60.](#) Mergulhao, L.P., Mohan, R., Murty, V.S.N., Guptha, M.V.S. and Sinha, D.K.:  
1012 Coccolithophores from the central Arabian Sea: Sediment trap results, *Journal of earth*  
1013 *system science*, 115, 415–428, <https://doi.org/10.1007/BF02702870>, 2006.
- 1014 [52-61.](#) [Meyers, P.A.: Organic geochemical proxies of paleoceanographic,](#)  
1015 [paleolimnologic, and paleoclimatic processes, \*Organic geochemistry\*, 27\(5–6\), 213–](#)  
1016 [250, \[https://doi.org/10.1016/S0146-6380\\(97\\)00049-1\]\(https://doi.org/10.1016/S0146-6380\(97\)00049-1\), 1997.](#)
- 1017 [53-62.](#) Moriceau, B., Iversen, M.H., Gallinari, M., Evertsen, A.J.O., Le Goff, M.,  
1018 Beker, B., Boutorh, J., Corvaisier, R., Coffineau, N., Donval, A. and Giering, S.L.,  
1019 Copepods boost the production but reduce the carbon export efficiency by diatoms,  
1020 *Frontiers in Marine Science*, 5, 82, <https://doi.org/10.3389/fmars.2018.00082>, 2018.
- 1021 [54-63.](#) Müller, J., Wagner, A., Fahl, K., Stein, R., Prange, M. and Lohmann, G.:  
1022 Towards quantitative sea ice reconstructions in the northern North Atlantic: A  
1023 combined biomarker and numerical modelling approach, *Earth and Planetary Science*  
1024 *Letters*, 306(3-4), 137–148, <https://doi.org/10.1016/j.epsl.2011.04.011>, 2011.
- 1025 [55-64.](#) Nair, R.R., Ittekkot, V., Manganini, S.J., Ramaswamy, V., Haake, B., Degens,  
1026 E.T., Desai, B.T. and Honjo, S.: Increased particle flux to the deep ocean related to  
1027 monsoons, *Nature*, 338(6218), 749–751, <https://doi.org/10.1038/338749a0>, 1989.
- 1028 [56-65.](#) Nomaki, H., Rastelli, E., Ogawa, N.O., Matsui, Y., Tsuchiya, M., Manea, E.,  
1029 Corinaldesi, C., Hirai, M., Ohkouchi, N., Danovaro, R. and Nunoura, T.: In situ  
1030 experimental evidences for responses of abyssal benthic biota to shifts in phytodetritus  
1031 compositions linked to global climate change, *Global Change Biology*, 27(23), 6139–  
1032 6155, <https://doi.org/10.1111/gcb.15882>, 2021.
- 1033 [57-66.](#) Pandey, M., Biswas, H. and Chowdhury, M.: Interlinking diatom frustule  
1034 diversity from the abyss of the central Arabian Sea to surface processes: physical  
1035 forcing and oxygen minimum zone, *Environmental Monitoring and*  
1036 *Assessment*, 195(1), 161, <https://doi.org/10.1007/s10661-022-10749-7>, 2023.
- 1037 [67.](#) Pandey, M. and Biswas, H.: May. An account of the key diatom frustules from the  
1038 surface sediments of the Central and Eastern Arabian Sea and their biogeochemical  
1039 significance, In *EGU General Assembly Conference Abstracts (EGU-131)*,  
1040 <https://doi.org/10.5194/egusphere-egu23-131>, 2023.
- 1041 [58-68.](#) [Pandey, Medhavi; Biswas, Haimanti; Birgel, Daniel; Burdanowitz, Nicole;](#)  
1042 [Gaye, Birgit, “Understanding biological carbon pump in the central Arabian Sea using](#)  
1043 [phytoplankton biomarkers and diatom frustules from surface sediments.”, \*Mendeley\*](#)  
1044 [Data, V1, doi: 10.17632/xm4nxzdx2.1, 2024.](#)
- 1045 [59-69.](#) Peng, P., Bi, R., Sachs, J.P., Shi, J., Luo, Y., Chen, W., Huh, C.A., Yu, M., Cao,  
1046 Y., Wang, Y. and Cao, Z.: Phytoplankton community changes in a coastal upwelling  
1047 system during the last century, *Global and Planetary Change*, 224, 104101,  
1048 <https://doi.org/10.1016/j.gloplacha.2023.104101>, 2023.
- 1049 [60-70.](#) Prah, F. G., Muehlhausen, L. A. and Zahnle, D. L.: Further evaluation of long-  
1050 chain alkenones as indicators of paleoceanographic conditions, *Geochim. Cosmochim.*  
1051 *Acta*, 52(9), 2303–2310, doi:10.1016/0016-7037(88)90132-9, 1988.
- 1052 [71.](#) Prah, F.G., Dymond, J. and Sparrow, M.A.: Annual biomarker record for export  
1053 production in the central Arabian Sea, *Deep Sea Research Part II: Topical Studies in*  
1054 *Oceanography*, 47(7-8), 1581–1604, [https://doi.org/10.1016/S0967-0645\(99\)00155-1](https://doi.org/10.1016/S0967-0645(99)00155-1),  
1055 2000.
- 1056 [61-72.](#) [Prah, F.G. and Wakeham, S.G.: Calibration of unsaturation patterns in long-](#)  
1057 [chain ketone compositions for palaeotemperature assessment, \*Nature\*, 330\(6146\),](#)  
1058 [pp.367-369, <https://doi.org/10.1038/330367a0>, 1987.](#)
- 1059 [62-73.](#) Prasanna Kumar S., Madhupratap, M., Kumar, M.D., Gauns, M.,  
1060 Muraleedharan, P.M., Sarma, V.V.S.S. and De Souza, S.N.: Physical control of primary

1061 productivity on a seasonal scale in central and eastern Arabian Sea, *Journal of Earth*  
1062 *System Science*, 109, 433–441, <https://doi.org/10.1007/BF02708331>, 2000.

1063 63-74. \_\_\_ Prasanna Kumar. S., and Narvekar, J.: Seasonal variability of the mixed layer  
1064 in the central Arabian Sea and its implication on nutrients and primary  
1065 productivity, *Deep Sea Research Part II: Topical Studies in Oceanography*, 52(14-15),  
1066 1848–1861, <https://doi.org/10.1016/j.dsr2.2005.06.002>, 2005.

1067 64-75. \_\_\_ Prasanna Kumar. S., Ramaiah, N., Gauns, M., Sarma, V.V.S.S., Muraleedharan,  
1068 P.M., Raghukumar, S., Kumar, M.D. and Madhupratap, M.: Physical forcing of  
1069 biological productivity in the Northern Arabian Sea during the Northeast  
1070 Monsoon, *Deep Sea Research Part II: Topical Studies in Oceanography*, 48(6-7), 1115–  
1071 1126, [https://doi.org/10.1016/S0967-0645\(00\)00133-8](https://doi.org/10.1016/S0967-0645(00)00133-8), 2001.

1072 65-76. \_\_\_ Ragueneau, O., Schultes, S., Bidle, K., Claquin, P. and Moriceau, B.: Si and C  
1073 interactions in the world ocean: Importance of ecological processes and implications  
1074 for the role of diatoms in the biological pump, *Global Biogeochemical Cycles*, 20(4),  
1075 <https://doi.org/10.1029/2006GB002688>, 2006.

1076 66-77. \_\_\_ Rixen, T., Gaye, B. and Emeis, K.C.: The monsoon, carbon fluxes, and the  
1077 organic carbon pump in the northern Indian Ocean, *Progress in oceanography*, 175, 24–  
1078 39, <https://doi.org/10.1016/j.pocean.2019.03.001>, 2019a.

1079 67-78. \_\_\_ Rixen, T., Gaye, B., Emeis, K.C. and Ramaswamy, V.: The ballast effect of  
1080 lithogenic matter and its influences on the carbon fluxes in the Indian Ocean,  
1081 *Biogeosciences*, 16(2), 485–503, <https://doi.org/10.5194/bg-16-485-2019>, 2019b.

1082 68-79. \_\_\_ Rodríguez-Miret, X., del Carmen Trapote, M., Sigró, J. and Vegas-Vilarrúbia,  
1083 T.: Diatom responses to warming, heavy rains and human impact in a Mediterranean  
1084 lake since the preindustrial period, *Science of The Total Environment*, 884, 163685,  
1085 <https://doi.org/10.1016/j.scitotenv.2023.163685>, 2023.

1086 69-80. \_\_\_ Roubeix, V., Becquevort, S. and Lancelot, C.: Influence of bacteria and salinity  
1087 on diatom biogenic silica dissolution in estuarine systems, *Biogeochemistry*, 88, 47–  
1088 62, <https://doi.org/10.1007/s10533-008-9193-8>, 2008.

1089 70-81. \_\_\_ Roxy, M. K., Modi, A., Murtugudde, R., Valsala, V., Panickal, S., Kumar, S.  
1090 P., Ravichandran, M., Vichi, M., and Levy, M.: A reduction in marine primary  
1091 productivity driven by rapid warming over the tropical Indian Ocean, *Geophysical*  
1092 *Research Letters*, 43, 826–833, <https://doi.org/10.1002/2015GL066979>, 2016.

1093 71-82. \_\_\_ Ryderheim, F., Grønning, J. and Kiørboe, T.: Thicker shells reduce copepod  
1094 grazing on diatoms, *Limnology and Oceanography Letters*, 7(5), 435–442,  
1095 <https://doi.org/10.1002/lol2.10243>, 2022.

1096 72-83. \_\_\_ Sawant, S. and Madhupratap, M.: Seasonality and composition of  
1097 phytoplankton. *Current Science*, 71(11), 1996.

1098 73-84. \_\_\_ Schubert, C.J., Villanueva, J., Calvert, S.E., Cowie, G.L., Von Rad, U., Schulz,  
1099 H., Berner, U. and Erlenkeuser, H.: Stable phytoplankton community structure in the  
1100 Arabian Sea over the past 200,000 years, *Nature*, 394(6693), 563–566,  
1101 <https://doi.org/10.1038/29047>, 1998.

1102 74-85. \_\_\_ Schulte, S., Mangelsdorf, K. and Rullkötter, J.: Organic matter preservation on  
1103 the Pakistan continental margin as revealed by biomarker geochemistry, *Organic*  
1104 *Geochemistry*, 31(10), 1005–1022, [https://doi.org/10.1016/S0146-6380\(00\)00108-X](https://doi.org/10.1016/S0146-6380(00)00108-X),  
1105 2000.

1106 75-86. \_\_\_ Schulte, S., Rostek, F., Bard, E., Rullkötter, J. and Marchal, O.: Variations of  
1107 oxygen-minimum and primary productivity recorded in sediments of the Arabian  
1108 Sea, *Earth and Planetary Science Letters*, 173(3), 205–221,  
1109 [https://doi.org/10.1016/S0012-821X\(99\)00232-0](https://doi.org/10.1016/S0012-821X(99)00232-0), 1999.

- 1110 [76.87.](#) Sharma, S., Ha, K.-J., Yamaguchi, R., Rodgers, K. B., Timmermann, A., and  
1111 Chung, E.: Future Indian Ocean warming patterns, *Nature Communications*, 14, 1789,  
1112 <https://doi.org/10.1038/s41467-023-37435-7>, 2023
- 1113 [77.88.](#) Silori, S., Sharma, D., Chowdhury, M., Biswas, H., Cardinal, D. and Mandeng-  
1114 Yogo, M.: Particulate organic matter dynamics and its isotopic signatures ( $\delta^{13}\text{C}_{\text{POC}}$   
1115 and  $\delta^{15}\text{N}_{\text{PN}}$ ) in relation to physical forcing in the central Arabian Sea during SW  
1116 monsoon (2017–2018), *Science of the Total Environment*, 785, 147326,  
1117 <https://doi.org/10.1016/j.scitotenv.2021.147326>, 2021.
- 1118 [78.89.](#) Singh, U.B. and Ahluwalia, A.S.: Microalgae: a promising tool for carbon  
1119 sequestration, *Mitigation and Adaptation Strategies for Global Change*, 18(1), 73–95,  
1120 <https://doi.org/10.1007/s11027-012-9393-3>, 2013.
- 1121 [79.90.](#) Smayda, T.J. and Reynolds, C.S.: Community assembly in marine  
1122 phytoplankton: application of recent models to harmful dinoflagellate blooms, *Journal*  
1123 *of plankton research*, 23(5), 447–461, <https://doi.org/10.1093/plankt/23.5.447>, 2001.
- 1124 [80.91.](#) Smetacek, V.S.: Role of sinking in diatom life-history cycles: ecological,  
1125 evolutionary and geological significance, *Marine biology*, 84, 239–251,  
1126 <https://doi.org/10.1007/BF00392493>, 1985.
- 1127 [81.92.](#) Smith, S., Roman, M., Prusova, I., Wishner, K., Gowing, M., Codispoti, L.A.,  
1128 Barber, R., Marra, J. and Flagg, C.: Seasonal response of zooplankton to monsoonal  
1129 reversals in the Arabian Sea, *Deep Sea Research Part II: Topical Studies in*  
1130 *Oceanography*, 45(10-11), 2369–2403, [https://doi.org/10.1016/S0967-0645\(98\)00075-](https://doi.org/10.1016/S0967-0645(98)00075-7)  
1131 [7](#), 1998.
- 1132 [82.93.](#) Sonzogni, C., Bard, E., Rostek, F., Lafont, R., Rosell-Mele, A. and Eglinton,  
1133 G.: Core-top calibration of the alkenone index vs sea surface temperature in the Indian  
1134 Ocean, *Deep Sea Res. Part II Top. Stud. Oceanogr.*, 44(6), 1445–1460,  
1135 doi:10.1016/S0967-0645(97)00010-6, 1997.
- 1136 [83.94.](#) Stoecker, D.K.: Mixotrophy among Dinoflagellates 1. *Journal of eukaryotic*  
1137 *microbiology*, 46, 397-401, <https://doi.org/10.1111/j.1550-7408.1999.tb04619.x>, 1999.
- 1138 [84.95.](#) Stoecker, D.K., Hansen, P.J., Caron, D.A. and Mitra, A.: Mixotrophy in the  
1139 marine plankton, *Annual Review of Marine Science*, 9, 311–335,  
1140 <https://doi.org/10.1146/annurev-marine-010816-060617>, 2017.
- 1141 [96.](#) Swanberg, N.R., and Anderson, O.R.: The nutrition of radiolarians: Trophic activity of  
1142 some solitary Spumellaria 1, *Limnology and Oceanography*, 30, 646–652,  
1143 <https://doi.org/10.4319/lo.1985.30.3.0646>, 1985.
- 1144 [85.97.](#) Taipale, S. J., Hiltunen, M, Vuorio, K., and Peltomaa, E., [Suitability of](#)  
1145 [Phytosterols Alongside Fatty Acids as Chemotaxonomic Biomarkers for](#)  
1146 [Phytoplankton. Front. Plant Sci. 7:212. doi: 10.3389/fpls.2016.00212, 2016.](#)
- 1147 [86.98.](#) Tarran, G.A., Burkill, P.H., Edwards, E.S. and Woodward, E.M.S.:  
1148 Phytoplankton community structure in the Arabian Sea during and after the SW  
1149 monsoon, 1994, *Deep Sea Research Part II: Topical Studies in Oceanography*, 46, 655–  
1150 676, [https://doi.org/10.1016/S0967-0645\(98\)00122-2](https://doi.org/10.1016/S0967-0645(98)00122-2), 1999.
- 1151 [87.99.](#) Ter Braak, C.J. and Smilauer, P.: CANOCO reference manual and CanoDraw  
1152 for Windows user's guide: software for canonical community ordination (version 4.5),  
1153 www.canoco.com, 2002.
- 1154 [88.100.](#) Tomas, C. R., (Ed.), *Identifying marine phytoplankton*. Elsevier, 1997.
- 1155 [89.101.](#) Tréguer, P., Bowler, C., Moriceau, B., Dutkiewicz, S., Gehlen, M., Aumont, O.,  
1156 Bittner, L., Dugdale, R., Finkel, Z., Iudicone, D. and Jahn, O.: Influence of diatom  
1157 diversity on the ocean biological carbon pump, *Nature Geoscience*, 11, 27–37,  
1158 <https://doi.org/10.1038/s41561-017-0028-x>, 2018.
- 1159 [102.](#) Vallivattathillam, P., Lachkar, Z. and Lévy, M.: Shrinking of the Arabian Sea  
1160 oxygen minimum zone with climate change projected with a downscaled



- 1161 model, *Frontiers in Marine Science*, 10, 1123739,  
1162 <https://doi.org/10.3389/fmars.2023.1123739>, 2023.
- 1163 ~~90-103.~~ Véron, B., Dauguet, J. C., & Billard, C. Sterolic biomarkers in marine  
1164 phytoplankton. II. Free and conjugated sterols of seven species used in mariculture.  
1165 *Journal of phycology*, 34(2), 273-279. [https://doi.org/10.1046/j.1529-](https://doi.org/10.1046/j.1529-8817.1998.340273.x)  
1166 [8817.1998.340273.x](https://doi.org/10.1046/j.1529-8817.1998.340273.x), 1998.
- 1167 ~~104.~~ Volk, T. and Hoffert, M.I.: Ocean carbon pumps: Analysis of relative strengths  
1168 and efficiencies in ocean-driven atmospheric CO<sub>2</sub> changes, *The carbon cycle and*  
1169 *atmospheric CO<sub>2</sub>: Natural variations Archean to present*, 32, 99–110,  
1170 <https://doi.org/10.1029/GM032p0099>, 1985.
- 1171 ~~105.~~ Volkman, J.K., Barrett, S.M., Blackburn, S.I., Mansour, M.P., Sikes, E.L. and  
1172 Gelin, F.: Microalgal biomarkers: a review of recent research developments. *Organic*  
1173 *Geochemistry*, 29(5-7), 1163-1179, [https://doi.org/10.1016/S0146-6380\(98\)00062-X](https://doi.org/10.1016/S0146-6380(98)00062-X),  
1174 1998.
- 1175 ~~91-106.~~ Volkman, J.: Sterols in microorganisms. *Applied microbiology and*  
1176 *Biotechnology*, 60, 495-506, <https://doi.org/10.1007/s00253-002-1172-8>, 2003.
- 1177 ~~92-107.~~ Wakeham, S.G., Peterson, M.L., Hedges, J.I. and Lee, C.: Lipid biomarker  
1178 fluxes in the Arabian Sea, with a comparison to the equatorial Pacific Ocean. *Deep Sea*  
1179 *Research Part II: Topical Studies in Oceanography*, 49, 2265–2301,  
1180 [https://doi.org/10.1016/S0967-0645\(02\)00037-1](https://doi.org/10.1016/S0967-0645(02)00037-1), 2002.
- 1181 ~~93-108.~~ Ward, B.B., Devol, A.H., Rich, J.J., Chang, B.X., Bulow, S.E., Naik, H.,  
1182 Pratihary, A. and Jayakumar, A.: Denitrification as the dominant nitrogen loss process  
1183 in the Arabian Sea, *Nature*, 461, 78–81, <https://doi.org/10.1038/nature08276>, 2009.
- 1184 ~~94-109.~~ Wishner, K.F., Gowing, M.M. and Gelfman, C.: Mesozooplankton biomass in  
1185 the upper 1000 m in the Arabian Sea: overall seasonal and geographic patterns, and  
1186 relationship to oxygen gradients, *Deep Sea Research Part II: Topical Studies in*  
1187 *Oceanography*, 45, 2405–2432, [https://doi.org/10.1016/S0967-0645\(98\)00078-2](https://doi.org/10.1016/S0967-0645(98)00078-2),  
1188 1998.
- 1189 ~~95-110.~~ Wittenborn, A.K., Schmale, O. and Thiel, V.: Zooplankton impact on lipid  
1190 biomarkers in water column vs. surface sediments of the stratified Eastern Gotland  
1191 Basin (Central Baltic Sea), *Plos one*, 15, e0234110,  
1192 <https://doi.org/10.1371/journal.pone.0234110>, 2020.
- 1193 ~~96-111.~~ Xiong, W., Mei, X., Meng, X., Chen, H. and Yang, H.: Phytoplankton  
1194 biomarkers in surface sediments from Liaodong Bay and their potential as indicators of  
1195 primary productivity, *Marine Pollution Bulletin*, 159, 111536,  
1196 <https://doi.org/10.1016/j.marpolbul.2020.111536>, 2020.
- 1197 ~~97-112.~~ Zúñiga, D., Sanchez-Vidal, A., Flexas, M.D.M., Carroll, D., Rufino, M.M.,  
1198 Spreen, G., Calafat, A. and Abrantes, F.: Sinking diatom assemblages as a key driver  
1199 for deep carbon and silicon export in the Scotia Sea (Southern Ocean), *Frontiers in*  
1200 *Earth Science*, 9, 579198, <https://doi.org/10.3389/feart.2021.579198>, 2021.

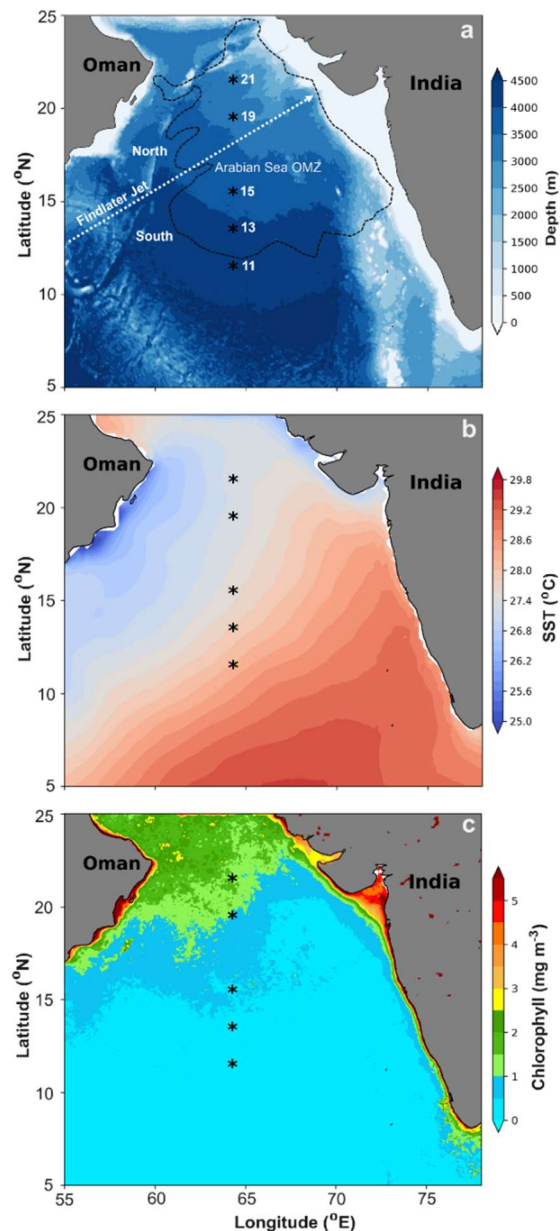
1201

1202

1203

1204

1205



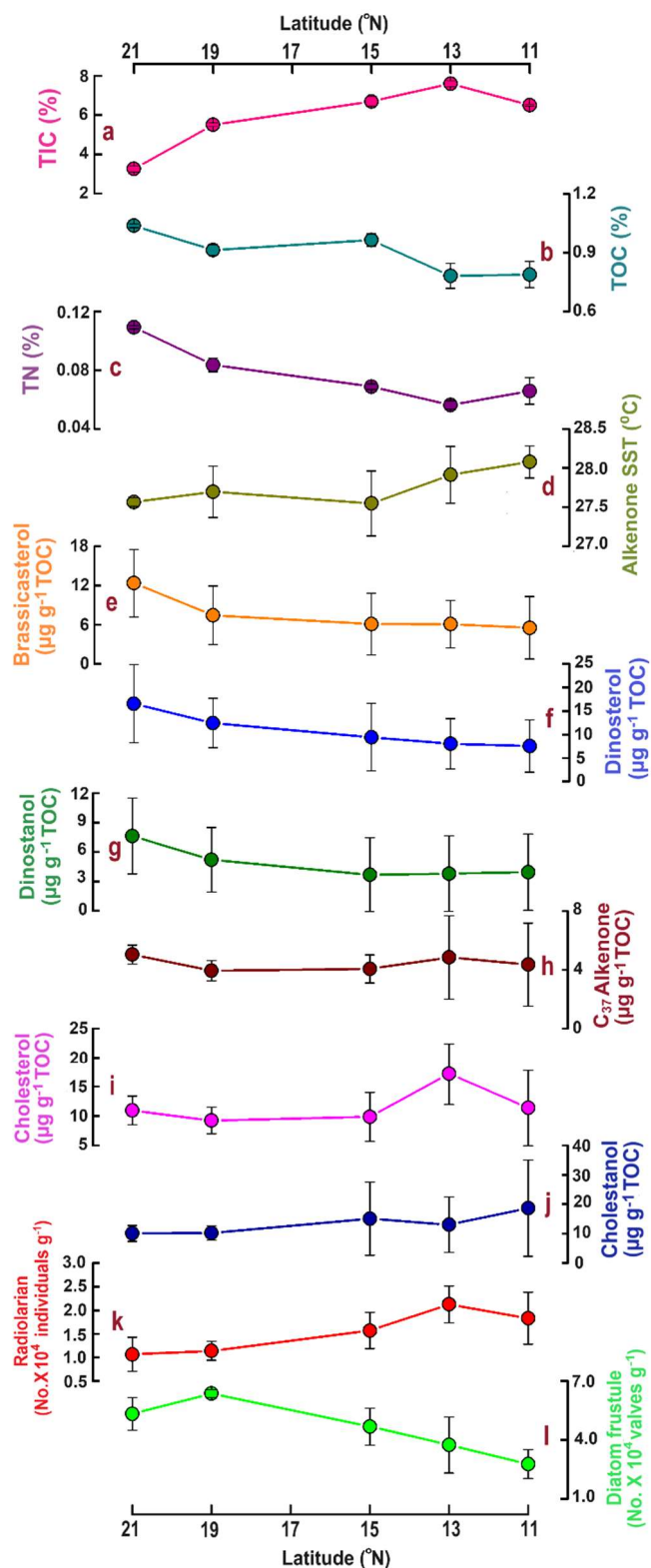
1207

1208

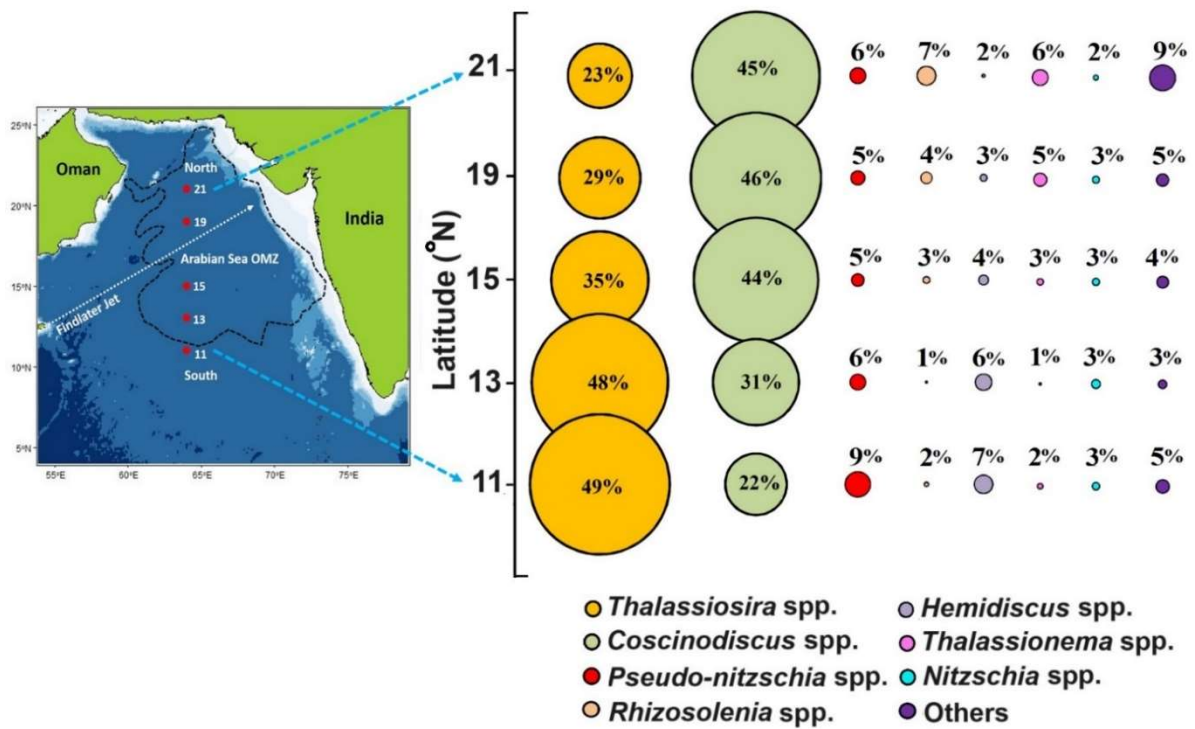
1209 **Figure 1. a)** Map showing the study locations in the Central Arabian Sea along 64° E transect  
 1210 during SSD-068 (Dec 2019) (a). The low-level atmospheric jet (Findlater Jet) is shown by a  
 1211 white dashed arrow and the boundary of the Oxygen Minimum Zone (OMZ) ( $0.5 \text{ mmol L}^{-1} \text{ O}_2$   
 1212 concentration) is shown by a black dashed line; b) The average SST (2017-2020) values  
 1213 depicting spatial variability among the sampling stations from the north to south (b); c) average  
 1214 Chla values derived from the satellite during for the time period 2017-2020 over the Arabian  
 1215 sea, indicating average phytoplankton biomass remains higher on an annual scale for the  
 1216 stations in the north compared to the south.

1217

1218  
 1219  
 1220  
 1221  
 1222  
 1223  
 1224  
 1225  
 1226  
 1227  
 1228  
 1229  
 1230  
 1231  
 1232  
 1233  
 1234  
 1235  
 1236  
 1237  
 1238  
 1239  
 1240  
 1241  
 1242  
 1243  
 1244  
 1245



1246 **Figure 2.** The distribution of total inorganic carbon (TIC %) (a), total organic carbon (TOC %) (b), total nitrogen (TN%) (c), alkenone based sea surface temperature (SST °C) (d),  
 1247  
 1248 brassicasterol (e), dinosterol (f), dinostanol (g), C<sub>37</sub> alkenones (h), cholesterol (i), cholestanol  
 1249 (j), radiolarians (k), and diatom frustules (l) along the 64° E transect in the central Arabian Sea.



1251

1252

1253

1254 **Figure 3.** The bubble plot shows the relative percentage of diatom frustules of major species  
 1255 (>3% of total abundance) from surface sediment samples (average of 0 – 0.5 cm and 0.5 - top  
 1256 0.5-1 cm) along the 64° E transect in the central Arabian Sea. Individual contributions from  
 1257 centric and pennate diatoms <3% were summed as “others”. The colors denote the specific  
 1258 phytoplankton taxa as indicated by colored closed circle at the bottom of the panel.

1259

1260

1261

1262

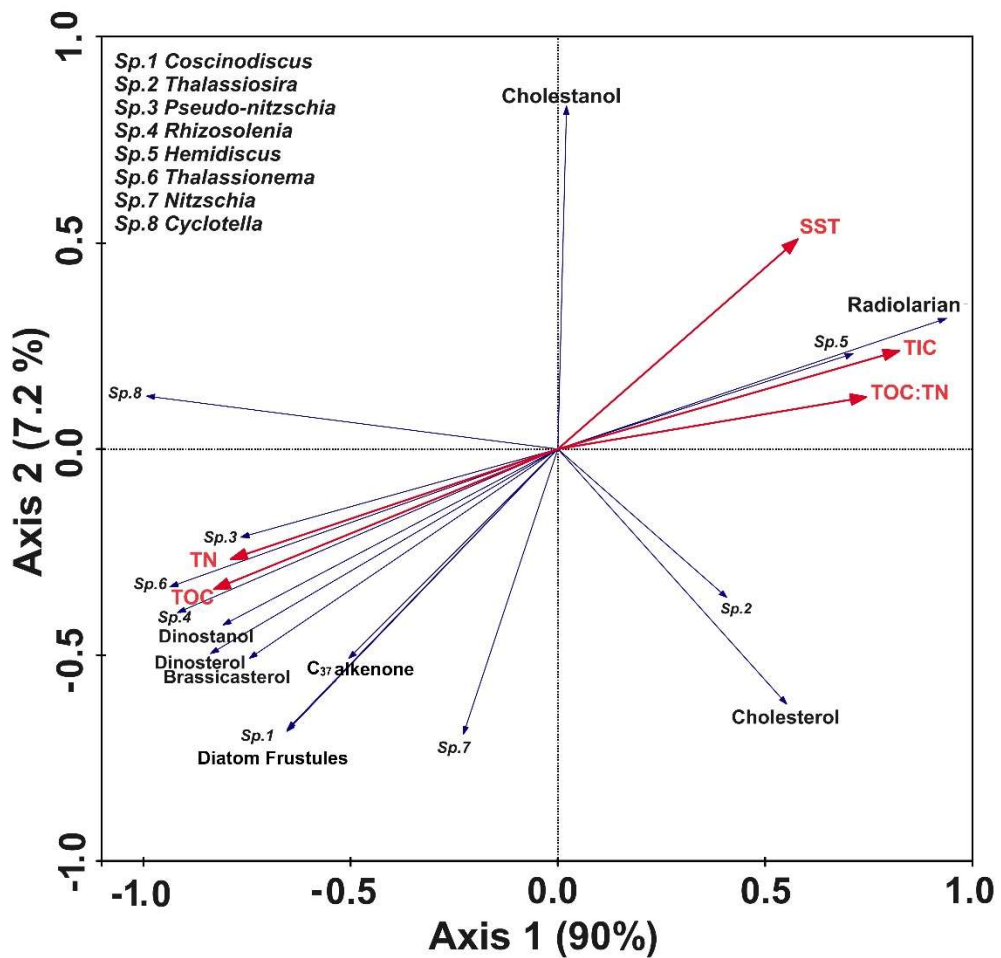
1263

1264

1265

1266

1267



1268

1269

1270 **Figure 4.** RDA biplot shows the interrelationship between the biotic key parameters shown in  
 1271 blue (diatom frustules, biomarkers, radiolarians) and bulk sedimentary parameter indicated in  
 1272 red abiotic factors (TOC; TN, TIC, TOC:TN; SST). The names of diatoms genera are marked  
 1273 as “Sp.” and are mentioned in the top left side of the panel. Axis 1 and axis 2 explained nearly  
 1274 97.2% of the variability.

1275

1276

1277

1278

1279

1280

1281

1282

1283

1284

1285

1286

1287

1288

1289

1290

1291

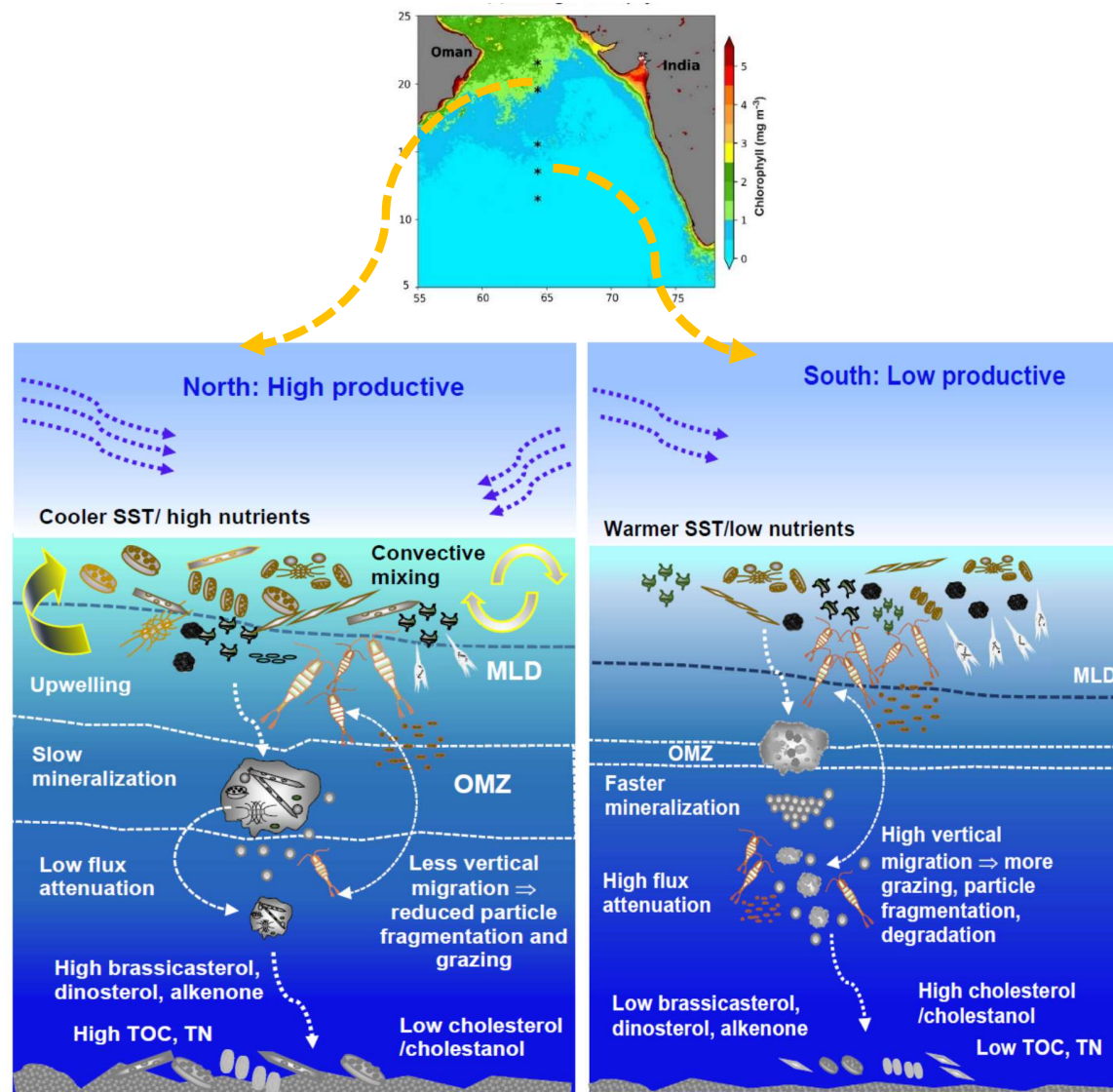
1292

1293

1294

1295

1296



1297

**Figure 5.** The schematic shows the spatial variability in particle flux along the 64° E transect in the central Arabian Sea.

1298 **Table 1.** Sedimentary characteristics, diatom frustules, and sterol concentrations in the surface sediments from the central Arabian Sea  
 1299 (n =2±SD). The values represent the average from 0.5 and 1 cm core slices.

<b>Latitude (°N)</b>	<b>21°</b>	<b>19°</b>	<b>15°</b>	<b>13°</b>	<b>11°</b>	<b>Average ±SD</b>
<b>TIC %</b>	3.25±0.15	5.50±0.09	6.70±0.24	7.60±0.13	6.51±0.06	5.91±1.66
<b>TOC %</b>	1.04±0.01	0.91±0.03	0.96±0.03	0.78±0.06	0.79±0.07	0.90±0.11
<b>TN %</b>	0.11±0.001	0.08±0.005	0.07±0.002	0.06±0.003	0.07±0.009	0.08±0.02
<b>TOC:TN</b>	9.5±0.18	10.9±0.28	14±0.08	13.9±1.83	12.1±2.69	12.1±1.9
<b>Alkenone based SST (°C)</b>	27.6±0.05	27.7±0.33	27.5±0.42	27.9±0.36	28.1±0.20	27.8±0.2
<b>Diatom frustule (No.×10<sup>4</sup> valves g<sup>-1</sup>)</b>	5.33±0.83	6.36±0.20	4.69±0.94	3.75±1.43	2.78±0.73	4.58±1.39
<b>Radiolarian (No.×10<sup>4</sup> individuals g<sup>-1</sup>)</b>	1.07±0.36	1.14±0.20	1.57±0.38	2.13±0.39	1.83±0.55	1.54±0.45
<b>Brassicasterol (ng g<sup>-1</sup>)</b>	128.0±52.6	68.6±43.0	58.2±43.5	46.4±24.4	42.0±33.9	68.62±34.77
<b>Dinosterol (ng g<sup>-1</sup>)</b>	171.1±84.4	114.2±51.4	89.8±66.2	61.0±36.7	57.7±38.8	98.76±46.53
<b>Dinostanol (ng g<sup>-1</sup>)</b>	79.0±39.4	48.0±31.5	34.7±35.2	28.3±27.8	29.8±28.0	43.95±21.05
<b>C<sub>37</sub> alkenone (ng g<sup>-1</sup>)</b>	52.2±6.3	36.0±7.4	39.0±8.0	36.9±19.1	33.3±19.3	39.47±7.39
<b>Cholesterol (ng g<sup>-1</sup>)</b>	113.2±24.4	84.4±23.3	94.1±36.8	132.3±29.5	87.3±42.9	102.27±20.21
<b>Cholestanol (ng g<sup>-1</sup>)</b>	104.4±26.9	93.7±24.6	143.5±115.1	98.6±65.3	141.6±116.5	116.37±24.22
<b>Dinosterol: Brassicasterol</b>	1.31	1.78	1.55	1.28	1.49	1.5±0.2
<b>Brassicasterol: Alkenone</b>	2.41	1.82	1.41	1.25	1.16	1.6±0.5

1300

1301

1302 **Table 2.** Average values of various parameters (n =2, ±SD) from the northern (21, 19, and 15° N) and southern stations (13 and 11° N)  
 1303 of the central Arabian Sea. The values shown in **bold “p”** represent the level of significance (single-factor ANOVA at 95% confidence  
 1304 level) between the northern and the southern stations.

1305

Parameter	North	South	<i>p</i> -value
<b>Total Inorganic Carbon (TIC %)</b>	5.15±1.57	7.06±0.63	<b>0.05</b>
<b>Total Organic Carbon (TOC %)</b>	0.97±0.06	0.78±0.05	<b>0.0009</b>
<b>Total Nitrogen (TN %)</b>	0.087±0.018	0.061±0.008	<b>0.03</b>
<b>Alkenone derived SST (°C)</b>	27.6±0.25	28.0±0.26	<b>0.043</b>
<b>Brassicasterol (µg g<sup>-1</sup> TOC)</b>	8.64±4.75	5.81±3.48	0.3
<b>Dinosterol (µg g<sup>-1</sup> TOC)</b>	12.81±6.30	7.80±4.47	0.2
<b>Dinostanol (µg g<sup>-1</sup> TOC)</b>	5.50±3.35	3.87±3.17	0.46
<b>C<sub>37</sub> alkenone (µg g<sup>-1</sup> TOC)</b>	4.34±0.81	4.60±2.33	0.8
<b>Cholesterol (µg g<sup>-1</sup> TOC)</b>	9.99±2.50	14.26±5.83	0.14
<b>Cholestanol (µg g<sup>-1</sup> TOC)</b>	11.80±6.33	15.85±11.39	0.49
<b>Dinosterol: Brassicasterol</b>	1.55±0.27	1.39±0.21	0.34
<b>Brassicasterol: Alkenone</b>	1.88±0.76	1.21±0.21	0.13
<b>Diatom frustules (No.×10<sup>4</sup> valves g<sup>-1</sup>)</b>	5.46±0.95	3.26±1.08	<b>0.009</b>
<b>Radiolarian (No.×10<sup>4</sup> individuals g<sup>-1</sup>)</b>	1.26±0.35	1.98±0.43	<b>0.019</b>

1306